

36

**NATIONAL BUREAU OF STANDARDS REPORT**

8695

Calculation of Gamma Ray Dose From Rectangular  
Sources Using Harmonic Analysis

20000912 059

INFO QUALITY INSPECTED 4

**Reproduced From  
Best Available Copy**



U.S. DEPARTMENT OF COMMERCE  
NATIONAL BUREAU OF STANDARDS

**DISTRIBUTION STATEMENT A**  
Approved for Public Release  
Distribution Unlimited

## THE NATIONAL BUREAU OF STANDARDS

The National Bureau of Standards is a principal focal point in the Federal Government for assuring maximum application of the physical and engineering sciences to the advancement of technology in industry and commerce. Its responsibilities include development and maintenance of the national standards of measurement, and the provisions of means for making measurements consistent with those standards; determination of physical constants and properties of materials; development of methods for testing materials, mechanisms, and structures, and making such tests as may be necessary, particularly for government agencies; cooperation in the establishment of standard practices for incorporation in codes and specifications; advisory service to government agencies on scientific and technical problems; invention and development of devices to serve special needs of the Government; assistance to industry, business, and consumers in the development and acceptance of commercial standards and simplified trade practice recommendations; administration of programs in cooperation with United States business groups and standards organizations for the development of international standards of practice; and maintenance of a clearinghouse for the collection and dissemination of scientific, technical, and engineering information. The scope of the Bureau's activities is suggested in the following listing of its four Institutes and their organizational units.

**Institute for Basic Standards.** Applied Mathematics. Electricity. Metrology. Mechanics. Heat. Atomic Physics. Physical Chemistry. Laboratory Astrophysics.\* Radiation Physics. Radio Standards Laboratory.\* Radio Standards Physics; Radio Standards Engineering. Office of Standard Reference Data.

**Institute for Materials Research.** Analytical Chemistry. Polymers. Metallurgy. Inorganic Materials. Reactor Radiations. Cryogenics.\* Materials Evaluation Laboratory. Office of Standard Reference Materials.

**Institute for Applied Technology.** Building Research. Information Technology. Performance Test Development. Electronic Instrumentation. Textile and Apparel Technology Center. Technical Analysis. Office of Weights and Measures. Office of Engineering Standards. Office of Invention and Innovation. Office of Technical Resources. Clearinghouse for Federal Scientific and Technical Information.\*\*

**Central Radio Propagation Laboratory.\*** Ionospheric Telecommunications. Tropospheric Telecommunications. Space Environment Forecasting. Aeronomy.

---

\* Located at Boulder, Colorado 80301.

\*\* Located at 5285 Port Royal Road, Springfield, Virginia 22171.

# NATIONAL BUREAU OF STANDARDS REPORT

NBS PROJECT

NBS REPORT

23101-12-2310432  
23101-40-2310434

May 25, 1965

8695

## Calculation of Gamma Ray Dose From Rectangular Sources Using Harmonic Analysis \*

E. E. Morris and E. J. Moses  
Radiation Theory Section  
Radiation Physics Division

and

L. V. Spencer  
Ottawa University, Ottawa, Kansas

\*Work supported by funds from the Defense Atomic Support Agency and the Office of Civil Defense.

### IMPORTANT NOTICE

NATIONAL BUREAU OF STANDARDS REPORTS are usually preliminary or progress accounting documents intended for use within the Government. Before material in the reports is formally published it is subjected to additional evaluation and review. For this reason, the publication, reprinting, reproduction, or open-literature listing of this Report, either in whole or in part, is not authorized unless permission is obtained in writing from the Office of the Director, National Bureau of Standards, Washington, D.C. 20234. Such permission is not needed, however, by the Government agency for which the Report has been specifically prepared if that agency wishes to reproduce additional copies for its own use.



U.S. DEPARTMENT OF COMMERCE  
NATIONAL BUREAU OF STANDARDS

## Abstract

Techniques are developed for evaluating the detector response due to radiation from rectangularly shaped surfaces. The angular distribution of the radiation is represented as a series of elementary functions dependent on azimuth and obliquity. Calculations are then performed for specific rectangle shapes and detector positions using these functions. Sample results are given for a plane monodirectional source of 1.25 Mev gamma rays incident on a concrete scattering medium. These results are derived from more extensive tabulations contained in the report.

## I. Introduction

Many shielding problems require the evaluation of the response of a detector due to radiation emerging from rectangular areas. For example, in structure shielding, one frequently wants to know the dose in some location due to radiation coming from a wall or ceiling. Methods are developed in this report for evaluating the detector response when the angular distribution of the radiation emerging from the surface depends on both obliquity and azimuth. Briefly, the azimuthal dependence of the angular distribution is expanded in

---

a Fourier series and then the obliquity dependence of each Fourier coefficient is expanded in functions of  $\cos\theta$ . The procedure has two advantages: 1) The two expansions permit the geometry stage of the calculation to be separated from the penetration stage. 2) Large tabulations of detailed results are unnecessary since it is possible to represent the detector response for any complicated rectangle-detector configuration as a linear combination of detector responses for more elementary configurations.

Berger and Lamkin [1] have done calculations similar to those in this report for azimuthally independent angular distributions. They expanded the obliquity distributions into Legendre polynomials, and with these did calculations for specific geometries. Hubbell, Bach, and Lamkin [2] applied the Legendre function approach to the case of a detector located over one corner of a rectangular radiating surface. They prepared rather extensive tabulations of integrals over Legendre functions for a variety of rectangle shapes and detector heights.

Spencer [3], approximated (again for azimuthally independent angular distributions) rectangular surfaces by surfaces in the shape of circles or circular sectors. He then made use of cumulative integrals over the obliquity dependence to estimate the detector response. The method was easy to apply especially when only one

or two circles (or circular sectors) were needed to approximate the given rectangle.

Raso and Woolf [4] have calculated the response of detectors located opposite the center of rectangular steel barriers. Their results are for monodirectional beams of 1.25 Mev gamma radiation incident in planes perpendicular to the barrier and parallel to the short side of the rectangle. A few of their results were compared with results using the techniques in this paper, and satisfactory agreement was observed.

Most gamma ray penetration calculations for plane sources yield angular distributions for an infinite plane geometry. It is necessary to introduce a schematization which represents the rectangular geometry. This report assumes: 1) That the radiation emerges from an infinite plane surface, 2) that the angular distribution of the radiation is independent of the point of emergence, 3) that the detector is collimated to respond only to radiation coming from a finite rectangular area, and 4) that the radiation undergoes no interaction while traveling from the surface to the detector.

In Section II, the geometry on which all the calculations in this report are based is described and the integral for the detector response is stated. The expansion functions for the angular distributions are introduced and penetration coefficients (the expansion

coefficients for the angular distribution) and geometry coefficients (integrals over the expansion functions for particular rectangle-detector configurations) are defined. The geometry described in Section II seems specialized, but in Section III, rules are given by which general configurations can be expressed in terms of the basic one. Results of sample calculations for a monodirectional source of 1.25 Mev gamma rays incident on concrete barriers are given in Section IV. The results are based on the Monte Carlo data of Berger and Morris [5].

Two appendices are given at the end of the report. Appendix A describes the evaluation of the geometry coefficients and gives tables of coefficients for the basic rectangle-detector configuration described in Section II. Tables of penetration coefficients along with a discussion of their derivation from basic penetration data are given in Appendix B. Data are given for source energies of 1.25 Mev and 0.66 Mev. The 1.25 Mev data are for gamma rays incident on concrete slabs from plane monodirectional and plane isotropic sources. The 0.66 Mev data are for gamma rays from a plane monodirectional source incident on slabs of concrete and iron.

## II. Formulation and Evaluation of the Detector Response

The results in this report are based on a corner detector position in contrast to the center detector position used by Spencer in [3]. The geometry is illustrated in Fig. 1; the rectangle is located in the first quadrant of the xy-plane and the detector is on the z-axis. Two parameters are needed to describe the geometry. The first, the eccentricity, describes the shape of the rectangle and is defined by

$$\epsilon = \frac{w}{l} \quad (1)$$

where  $l$  and  $w$  are the x- and y-coordinates of the corner opposite the origin. The second is the solid angle fraction (solid angle in steradians divided by  $2\pi$ ) subtended at the detector by the rectangle and is given in terms of  $l$ ,  $w$ , and  $h$  (the z-coordinate of the detector) by

$$\omega = \frac{1}{2\pi} \tan^{-1} \left[ \frac{w l}{h \sqrt{h^2 + l^2 + w^2}} \right]. \quad (2)$$

Note that for a corner detector,  $\omega \leq 0.25$ .

If  $f(\theta, \varphi)$  represents the angular distribution of the flux emerging from the surface, then  $f(\theta, \varphi)d\Omega$  is the detector response due to radiation emerging from a differential area subtending a solid angle  $d\Omega = d(\cos\theta)d\varphi$  at the detector. The detector response due to the entire rectangular area is then given by the integral,

$$R = \int_{\cos\theta_1}^1 d(\cos\theta) \int_{\varphi_1}^{\varphi_2} d\varphi f(\theta, \varphi), \quad (3)$$

where the limits of integration must take account of the size and shape of the rectangle. An alternative way of writing the above integral makes use of a function  $G(\theta, \varphi, \epsilon, \omega)$  which has the property that  $G(\theta, \varphi, \epsilon, \omega) = 1$  when the direction  $(\theta, \varphi)$  corresponds to a point in the rectangle and  $G(\theta, \varphi, \epsilon, \omega) = 0$  otherwise. The function is a generalization of the response function defined in [1]. Using  $G(\theta, \varphi, \epsilon, \omega)$ , (3) may be written

$$R = \int_0^1 d(\cos\theta) \int_{-\pi}^{\pi} d\varphi f(\theta, \varphi) G(\theta, \varphi, \epsilon, \omega). \quad (4)$$

In Fig. 1, the azimuth  $\varphi = 0$  has been taken along one of the sides of the rectangle (the x-axis), but, it is conceivable that the angular distribution  $f(\theta, \varphi)$  will be symmetric about some other azimuth. Denoting this symmetry azimuth by  $\varphi_0$ , and assuming the angular distribution to be an even function of  $\varphi - \varphi_0$ , the azimuthal dependence may be expanded in a Fourier series:

$$f(\theta, \varphi - \varphi_0) = \sum_{m=0}^{\infty} f_m(\theta) \cos [m(\varphi - \varphi_0)]. \quad (5)$$

The integral for the detector response (4) may then be written

$$\begin{aligned} R &= \sum_{m=0}^{\infty} \int_0^1 d(\cos \theta) f_m(\theta) \int_{-\pi}^{\pi} d\varphi \cos [m(\varphi - \varphi_0)] G(\theta, \varphi, \epsilon, \omega) \\ &= \sum_{m=0}^{\infty} \cos m\varphi_0 \int_0^1 d(\cos \theta) f_m(\theta) \int_{-\pi}^{\pi} d\varphi \cos m\varphi G(\theta, \varphi, \epsilon, \omega) \\ &+ \sum_{m=1}^{\infty} \sin m\varphi_0 \int_0^1 d(\cos \theta) f_m(\theta) \int_{-\pi}^{\pi} d\varphi \sin m\varphi G(\theta, \varphi, \epsilon, \omega). \end{aligned} \quad (6)$$

In (6), the integrals over the azimuth depend only on the rectangle-detector configuration, but penetration and geometry are still linked together by the integrals over obliquity. Complete separation of the penetration stage of the problem from the geometry stage can be accomplished by expanding  $f_m(\theta)$  in a series of functions depending on  $\theta$ . The representation

$$f_m(\theta) = \sum_{i=0}^{\infty} f_{im} (1 - \cos \theta)^{i + \frac{m}{2}} \quad (7)$$

was chosen partly because of its simple form. The term  $m/2$  in the exponent was suggested by the associated Legendre functions and insures that

$$\lim_{\cos \theta \rightarrow 1} \sum_{i=0}^{\infty} f_{im} (1 - \cos \theta)^{i + \frac{m}{2}} = 0$$

when  $m > 0$ . In the remainder of this report, the coefficients  $f_{im}$  will be referred to as penetration coefficients.

Using (7), the expression for the detector response becomes

$$R = \sum_{m=0}^{\infty} \cos m\varphi_0 \sum_{i=0}^{\infty} f_{im} \int_0^1 d(\cos \theta) (1 - \cos \theta)^{i + \frac{m}{2}} \int_{-\pi}^{\pi} d\varphi \cos m\varphi G(\theta, \varphi, \epsilon, \omega) \\ + \sum_{m=0}^{\infty} \sin m\varphi_0 \sum_{i=0}^{\infty} f_{im} \int_0^1 d(\cos \theta) (1 - \cos \theta)^{i + \frac{m}{2}} \int_{-\pi}^{\pi} d\varphi \sin m\varphi G(\theta, \varphi, \epsilon, \omega). \quad (8)$$

Defining geometry coefficients,

$$G_{im}^e(\epsilon, \omega) = \int_0^1 d(\cos \theta) (1 - \cos \theta)^{i + \frac{m}{2}} \int_{-\pi}^{\pi} d\varphi \cos m\varphi G(\theta, \varphi, \epsilon, \omega),$$

$$G_{im}^o(\epsilon, \omega) = \int_0^1 d(\cos \theta) (1 - \cos \theta)^{i + \frac{m}{2}} \int_{-\pi}^{\pi} d\varphi \sin m\varphi G(\theta, \varphi, \epsilon, \omega), \quad (9)$$

(8) may be written

$$R = \sum_{m=0}^{\infty} \cos m\varphi_0 \sum_{i=0}^{\infty} f_{im} G_{im}^e(\epsilon, \omega)$$

$$+ \sum_{m=1}^{\infty} \sin m\varphi_0 \sum_{i=0}^{\infty} f_{im} G_{im}^o(\epsilon, \omega). \quad (10)$$

The desired result, separation of the penetration stage of the calculation from the geometrical stage, has been achieved in (10). Information about the source radiation is carried by the symmetry azimuth  $\varphi_0$  and the penetration coefficients  $f_{im}$ . The geometry coefficients depend only on the choice of expansion functions and on the size and shape of the rectangle relative to the detector.

### III. Arbitrary Detector Positions

The first step in applying the geometry coefficients to a given rectangle-detector configuration is to introduce a cartesian coordinate system with the rectangle in the  $xy$ -plane and the  $z$ -axis passing through the detector. The azimuth of symmetry may then be measured from the  $x$ -axis. This section demonstrates that arbitrary rectangle-detector configurations can be reduced to a series of problems involving rectangles in the first quadrant, as in Fig. 1, and that geometry coefficients are needed only for rectangles with eccentricities  $e \leq 1$ . These conclusions are a consequence of the following two general rules:

Rule 1. The detector response for a given rectangle and symmetry azimuth  $\varphi_0$  is unchanged if the rectangle and symmetry azimuth are rotated about the  $z$ -axis through an angle  $\alpha$  as illustrated in Fig. 2a (the line of sight in the figure is parallel to the  $z$ -axis). The symmetry azimuth for the rectangle after rotation is  $\varphi_0 + \alpha$ .

Rule 2. If a given rectangle and symmetry azimuth  $\varphi_0$  are reflected in any plane containing the z-axis, the detector response for the image rectangle is equivalent to the detector response for the original rectangle (Fig. 2b). The symmetry azimuth for the image rectangle is  $2\varphi_r - \varphi_0$  where  $\varphi_r$  is the azimuth of the reflecting plane.

As examples, consider the three off-corner detector positions illustrated in Fig. 3. It is usually convenient to take the x-axis parallel to one of the sides of the rectangle as is done in the figures. In each of the three cases, component rectangles can be defined; the i-th component rectangle has one corner at the origin and its opposite corner at the i-th corner of the basic rectangle. The detector response for the component rectangles in the first quadrant can be calculated using (10). Equation (10) can be used to calculate the detector response for those component rectangles not in the first quadrant if they are first rotated into the first quadrant following rule 1. Should a rectangle in the first quadrant have an eccentricity  $e > 1$ , the detector response can be calculated for its image when it is reflected in the plane  $\varphi = \pi/4$ .

The eccentricity for the image rectangle is  $\epsilon' = 1/\epsilon$  and, if the symmetry azimuth for the original rectangle is  $\varphi_0$ , the symmetry azimuth for the image rectangle is, according to rule 2,  $(\pi/2) - \varphi_0$ . Denoting the detector response for the  $i$ -th component rectangle in Figs. 3a, 3b, and 3c by  $R_i^{(a)}$ ,  $R_i^{(b)}$ , and  $R_i^{(c)}$  respectively, the detector responses for the basic rectangles are given by

$$R^{(a)} = R_1^{(a)} + R_2^{(a)} + R_3^{(a)} + R_4^{(a)}$$

$$R^{(b)} = R_1^{(b)} - R_2^{(b)} - R_3^{(b)} + R_4^{(b)}$$

$$R^{(c)} = R_1^{(c)} - R_2^{(c)} + R_3^{(c)} - R_4^{(c)}$$

A special case of the geometry in Fig. 3a has the detector located opposite the center of the rectangle, and is called a center detector position. If the  $x$ -axis is taken parallel to the long side of the rectangle, the expression for the detector response can be written in the explicit form

$$R = 4 \sum_{m=0}^{\infty} \cos 2m\varphi_0 \sum_{i=0}^{\infty} f_{i,2m} G_{i,2m}^e(\epsilon, \omega), \quad (11)$$

where  $\omega$  is the solid angle fraction subtended at the detector by one of the component rectangles and  $e$  is the width-to-length ratio of the rectangle. Equation (11) differs from (10) in one important respect. Terms involving  $f_{im}$  for odd values of  $m$  do not appear in (11). This has the consequence that for azimuthally dependent angular distributions, it is impossible to derive the detector response for one of the component rectangles from the response for a center detector position.

#### IV. An Illustration: Plane Monodirectional, 1.25 Mev Source Calculations

In this section, results of trial calculations for a source of 1.25 Mev gamma rays incident on concrete slabs are discussed. The normalization of the penetration coefficients is such that

$$\frac{D}{D_0} = \cos \theta_0 R \quad (12)$$

where  $R$  is given by either (10) or (11),  $\theta_0$  is the obliquity of the source radiation, and  $D/D_0$  is the ratio of the scattered dose rate (flux) reaching the detector to the dose rate (flux) incident on the scattering medium from the source. For a monodirectional source, the symmetry azimuth  $\varphi_0$  in (10) and (11) is

the azimuth of incidence.

Calculations using (12) and (10) have been compared with results obtained by integrating (3) numerically without expanding  $f(\theta, \varphi)$ . The sums in (10) were terminated after  $m = i = 4$ . The percent deviation of results using (12) and (10) from results obtained by direct numerical integration is given in Table 1 for a rectangle with thickness 1.0 mfp and eccentricity  $\epsilon = 0.5$  and for radiation incident with  $\cos\theta_0 = 0.5$ . In about 60 percent of the cases shown, the absolute deviation is less than 5 percent. None of the deviations in the table have absolute values greater than 15 percent. The results in the table are fairly representative of other transmission results. Exceptions are rectangles with very small eccentricity ( $\epsilon < 0.1$ ) where absolute deviations may be as large as 20 or 25 percent. For reflection, if  $\cos\theta_0 < 0.5$  and  $\omega \ll 0.1$ , absolute deviations in excess of 20 percent occur often. This is because for grazing angles of incidence, the reflected flux tends to peak strongly for large obliquities, thus causing (7) to converge slowly.

Figure 4 shows  $D/D_0$  for the rectangle-detector geometry of Fig. 1 as a function of the eccentricity  $\epsilon$  for several values of the solid angle fraction  $\omega$ . The results are for radiation

incident with  $\theta_0 = 60^\circ$ ,  $\varphi_0 = 0^\circ$ , and transmitted through a barrier 2.0 mfp thick. For large values of  $\omega$ , the detector response is nearly independent of the shape of the rectangle, but for smaller  $\omega$ 's, the response may vary by as much as 60 percent or more as the shape changes.

The response for a center detector position and the detector response for the component rectangle in the first quadrant are given in Fig. 5 as a function of the symmetry azimuth  $\varphi_0$ . The dashed curve represents the ratio  $D/D_0$  for the center detector position. Four times  $D/D_0$  for the component rectangle is given by the solid curve. The factor of four was included to make the magnitudes of the two quantities more nearly comparable.  $D/D_0$  for the center detector position has symmetry about not only  $\varphi_0 = 0$ , but also about  $\varphi_0 = \pi/2, \pi$ , and  $3\pi/2$ . In contrast, the detector response for the component rectangle does not exhibit symmetry about any  $\varphi_0$  in the range  $0 \leq \varphi_0 \leq 2\pi$ .

Mehlhorn, Clarke, Gold, and McMath [6] have carried out experiments with nearly monodirectional beams of  $^{60}\text{Co}$  radiation incident on square steel plates. The circles and triangles in Fig. 6 show results of measurements of  $D/D_0$  for a detector located under the corner of the plate and for radiation incident

with  $\theta_0 = 60^\circ$  and  $\psi_0 = 0^\circ$ . The experimental points all correspond to detector positions outside the direct beam. The solid curves show theoretical values for equivalent mass thicknesses of concrete. Where the experimental points show a definite trend with changing solid angle fraction, the trend agrees well with the theoretical trend. The discrepancy between the magnitudes of the experimental and theoretical values may be due to scattering from the floor and walls of the hole in which the detectors were located during the experiment.

#### V. Conclusions

One of the original goals for the work described in this report was to permit the estimation of the detector response for a rectangular barrier configuration by a fairly simple hand computation. Given the appropriate penetration and geometry coefficients, (10) is easy to evaluate by hand. However, in practice, hand computations may become rather tedious. For example, for a monodirectional source, the penetration coefficients depend on the source energy, source obliquity, and barrier thickness, while the geometry coefficients depend on the eccentricity and the solid angle fraction. Thus, the detector response may depend on as many as five variables. If it is necessary, in a given situation, to interpolate in one or more of these variables, (10) must be evaluated several times to get an

answer for a single rectangle shape and detector position. As a result, the geometry and penetration coefficients were placed on punched cards and a FORTRAN program was written to evaluate (10) and perform some of the necessary interpolations.

Acknowledgments: The authors wish to thank Mr. Charles Eisenhauer and Dr. Martin Berger for many helpful discussions during the course of this work.

## Appendix A

### Evaluation of the Geometry Coefficients

The geometry coefficients, defined by (9), were evaluated for the geometry of Fig. 1. To evaluate the integrals, it is necessary to replace  $G(\theta, \varphi, \epsilon, \omega)$  with appropriate limits on the range of integration. Regardless of the order in which the integrals are evaluated, the integral taken first can be evaluated analytically while the second must be evaluated numerically. The limits of integration are somewhat less complicated if the  $\cos\theta$ -integration is taken first. Then  $\Psi(\varphi, \epsilon, \omega) \leq \cos\theta \leq 1$  and  $0 \leq \varphi \leq \pi/2$  where  $\Psi(\varphi, \epsilon, \omega)$  is given by

$$\Psi(\varphi, \epsilon, \omega) = \frac{\eta \cos \varphi}{\sqrt{1 + \eta^2 \cos^2 \varphi}}, \quad \varphi \leq \tan^{-1} \epsilon;$$

$$\Psi(\varphi, \epsilon, \omega) = \frac{\eta \sin \varphi}{\sqrt{\epsilon^2 + \eta^2 \sin^2 \varphi}}, \quad \varphi > \tan^{-1} \epsilon.$$

$\eta$  is given in terms of  $\epsilon$  and  $\omega$  by

$$\eta = \frac{1}{\sqrt{2}} \left[ \sqrt{(1 + \epsilon^2)^2 + 4 \epsilon^2 \cot^2 2\pi \omega} - (1 + \epsilon^2) \right]^{\frac{1}{2}}.$$

In a given situation, it may be more convenient to evaluate  $\eta$  by the expression

$$\eta = \frac{h}{\ell}$$

where  $h$  is the detector height and  $\ell$  is the rectangle length.

Using the limits of integration, the expressions for the geometry coefficients become

$$G_{im}^e(\epsilon, \omega) = \int_0^{\pi/2} d\varphi \cos m\varphi \int_{\Psi(\varphi, \epsilon, \omega)}^1 d(\cos\theta) (1 - \cos\theta)^{i + \frac{m}{2}} ;$$

$$G_{im}^o(\epsilon, \omega) = \int_0^{\pi/2} d\varphi \sin m\varphi \int_{\Psi(\varphi, \epsilon, \omega)}^1 d(\cos\theta) (1 - \cos\theta)^{i + \frac{m}{2}} .$$

Evaluating the integral over  $\cos\theta$  gives

$$G_{im}^e(\epsilon, \omega) = \frac{1}{i + \frac{m}{2} + 1} \int_0^{\pi/2} d\varphi \cos m\varphi [1 - \Psi(\varphi, \epsilon, \omega)]^{i + \frac{m}{2} + 1} ;$$

$$G_{im}^o(\epsilon, \omega) = \frac{1}{i + \frac{m}{2} + 1} \int_0^{\pi/2} d\varphi \sin m\varphi [1 - \Psi(\varphi, \epsilon, \omega)]^{i + \frac{m}{2} + 1} .$$

---

Values of the geometry coefficients are given in Tables A1 through A9 for nine values of  $\epsilon$ , eight values of  $\omega$ , five values of  $l$ , and five values of  $m$ .

## Appendix B

The penetration coefficients defined in Section II were derived from the Monte Carlo data of Berger and Morris as follows: First, azimuthal expansion coefficients were computed using the formula

$$f_m(\theta) = \frac{2}{N} \left( \frac{1}{1 + \delta_{0m} + \delta_{Nm}} \right) \sum_{j=0}^N \left( \frac{1}{1 + \delta_{0j} + \delta_{Nj}} \right) \cos m \frac{j\pi}{N} f\left(\theta, \frac{j\pi}{N}\right),$$

where  $m \leq N$  and where  $N + 1$  is the number of evenly spaced azimuthal points for which the angular distributions were given. ( $\delta_{Nj}$  is the Kronecker  $\delta$  symbol). The coefficients computed using the above formula minimize the quantity

$$E_1(M, \theta) = \sum_{j=0}^N \left( \frac{1}{1 + \delta_{0j} + \delta_{Nj}} \right) \left[ f\left(\theta, \frac{j\pi}{N}\right) - \sum_{m=0}^M f_m(\theta) \cos m \frac{j\pi}{N} \right]^2,$$

for  $M < N$ . If  $M = N$ ,  $E_1(N, \theta) = 0$  [7].

Next, the penetration coefficients  $f_{im}$  were chosen to minimize

$$E_2(I, m) = \sum_{k=1}^K \left[ f_m(\theta_k) - \sum_{i=0}^I f_{im} (1 - \cos \theta_k)^{i + \frac{m}{2}} \right]^2,$$

where K is the number of obliquities for which the angular distributions were known and I + 1 is the number of terms in the expansion.

Penetration coefficient data for monoenergetic, plane monodirectional sources are given in Tables B1 through B8. The normalization for the penetration coefficients is given by (12). The data in Tables B1 through B6 pertain to 1.25 Mev gamma rays incident on concrete. For two incident directions, Table B7 contains data for 0.66 Mev gamma rays incident on concrete. Table B8 contains data for the same two directions for 0.66 Mev gamma rays incident on iron.

Table B9 gives penetration coefficients for a plane isotropic source of 1.25 Mev gamma rays with the source plane parallel to a concrete scattering medium. Coefficients are given for scattered radiation and for the total (scattered plus unscattered) transmitted radiation. The coefficients for the scattered radiation were obtained by integration of the 1.25 Mev monodirectional results. The normalization of the penetration coefficients is such that

$$D = E_0 \mu_d(E_0) \sigma \sum_{i=0}^I f_{i0} G_{i0}^e(\epsilon, \omega) ,$$

where D is the dose rate (flux) received at the detector,  $E_0$  is the source energy,  $\mu_d(E_0)$  is the energy transfer coefficient for air, and  $\sigma$  is the number of photons per second per  $\text{cm}^2$  emitted from the source plane in all directions.

## References

1. M. J. Berger and J. C. Lamkin, J. Research Natl. Bur. Standards 60, 109 (1958). RP2827.
2. J. H. Hubbell, R. L. Bach, and J. C. Lamkin, J. Research Natl. Bur. Standards 64C, 121 (1962).
3. L. V. Spencer, "Structure Shielding against Fallout Radiation from Nuclear Weapons", NBS Monograph 42 (1962).
4. D. J. Raso and S. Woolf, Technical Operations, Inc., Report No. TO-B 64-49 (June 1964).
5. M. J. Berger and E. E. Morris, unpublished.
6. H. A. Mehlhorn, E. T. Clarke, R. Gold, and R. McMath, Technical Operations, Inc., Report No. TO-B 62-13 (September 1962).
7. C. Lanczos, Applied Analysis, pp. 229-241 (Prentice Hall, Inc., Englewood Cliffs, New Jersey) (1956).

## Figure Captions

Fig. 1. Basic rectangle-detector geometry.

Fig. 2. (a) Rotation of a rectangle and symmetry azimuth through an angle  $\alpha$ .

(b) Reflection of a rectangle and symmetry azimuth through the plane  $\varphi = \varphi_r$ .

The projection of the detector on the  $xy$ -plane is shown at the origin.

Fig. 3. Three off-corner detector positions. Definition of component rectangles.

Fig. 4. Dependence of  $D/D_0$  on the eccentricity  $e$  for several values of the solid angle fraction  $\omega$ . Results shown are for a corner detector position, source energy  $E_0 = 1.25$  Mev,  $\theta_0 = 60^\circ$ ,  $\varphi_0 = 0^\circ$ , and a concrete scattering medium with thickness 2.0 mfp.

Fig. 5. Dashed curve shows  $D/D_0$  for a center detector position as a function of the symmetry azimuth  $\varphi_0$  when the rectangle subtends a solid angle fraction  $\omega = 0.4$ . Solid curve shows four times  $D/D_0$  for a corner detector position when the rectangle subtends a solid angle fraction  $\omega = 0.1$ . Both curves are for  $E_0 = 1.25$  Mev,  $\theta_0 = 60^\circ$ , and 1.0 mfp of concrete. The rectangle has eccentricity  $e = 0.5$ .

Figure Captions (Continued)

Fig. 6. Comparison with the experiment of Mehlhorn, et al. for a  $^{60}\text{Co}$  source of radiation incident with  $\theta_0 = 60^\circ$  and  $\varphi_0 = 0^\circ$  on steel plates with eccentricity  $\epsilon = 1.0$  and with the detector in a corner position. The circles and triangles represent experimental results for 1 inch and 2 inches of steel respectively. Curves (1) and (2) are calculated results for 1.11 mfp and 2.22 mfp of concrete respectively.

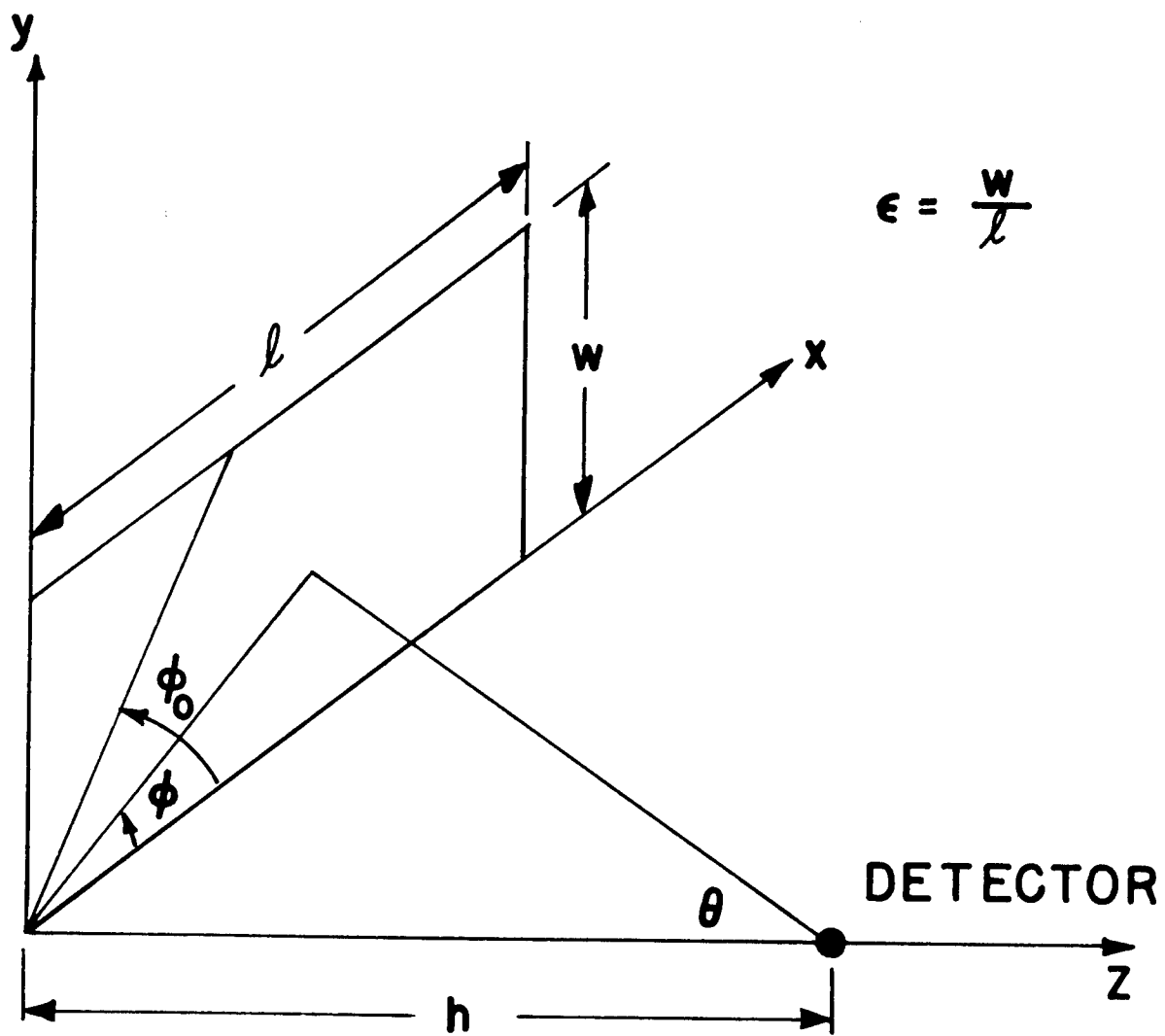


Figure 1

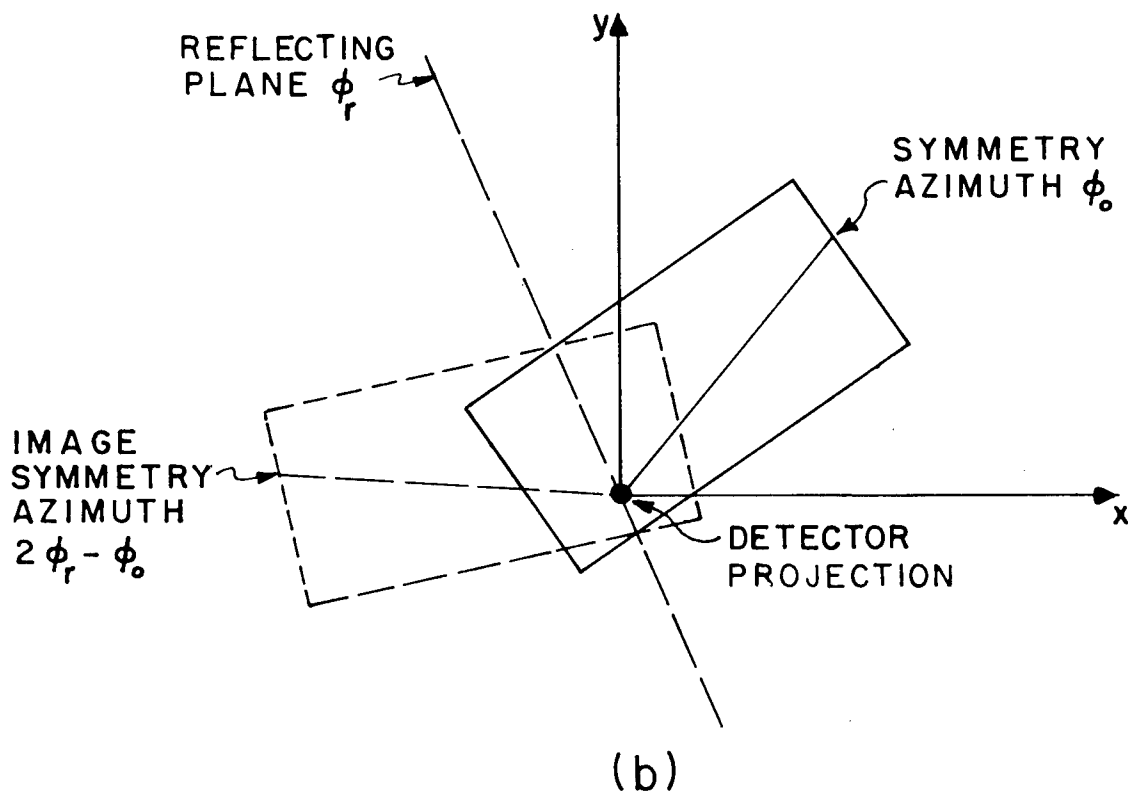
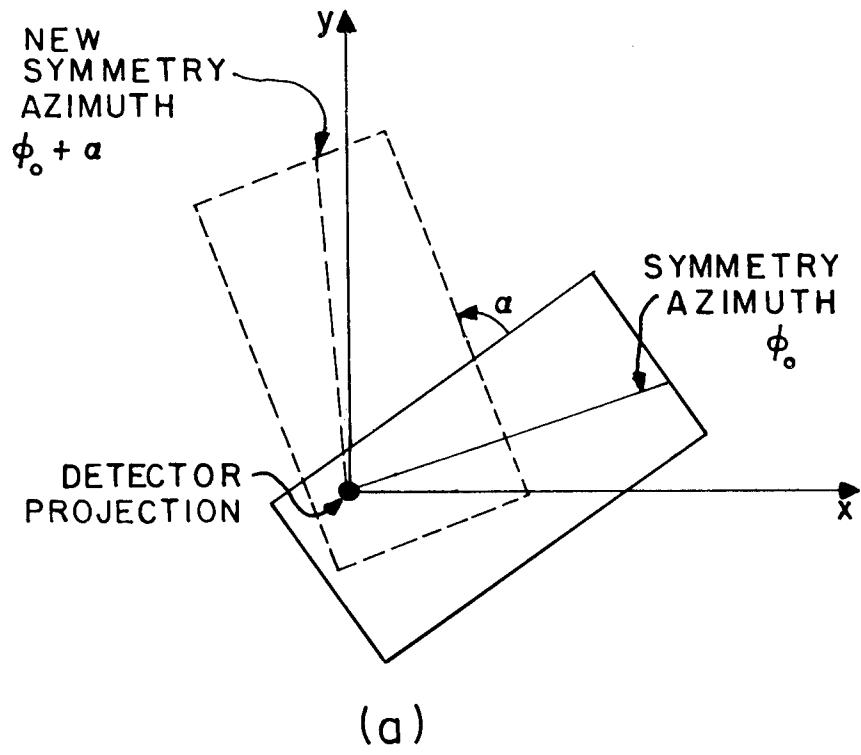


Figure 2

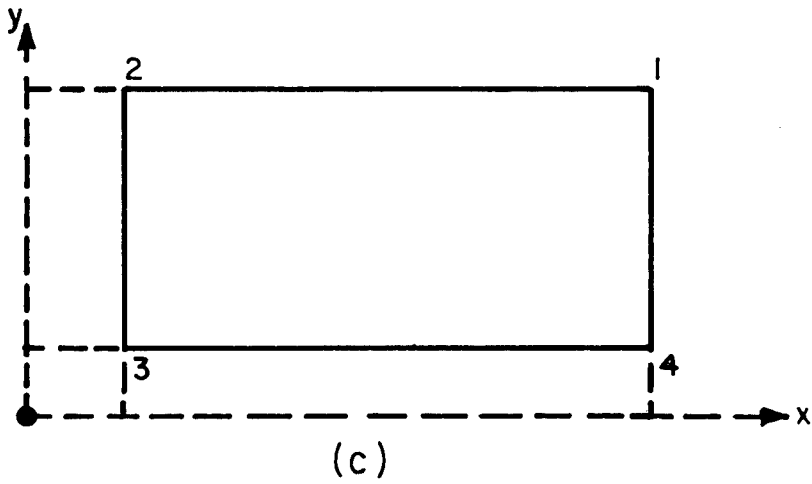
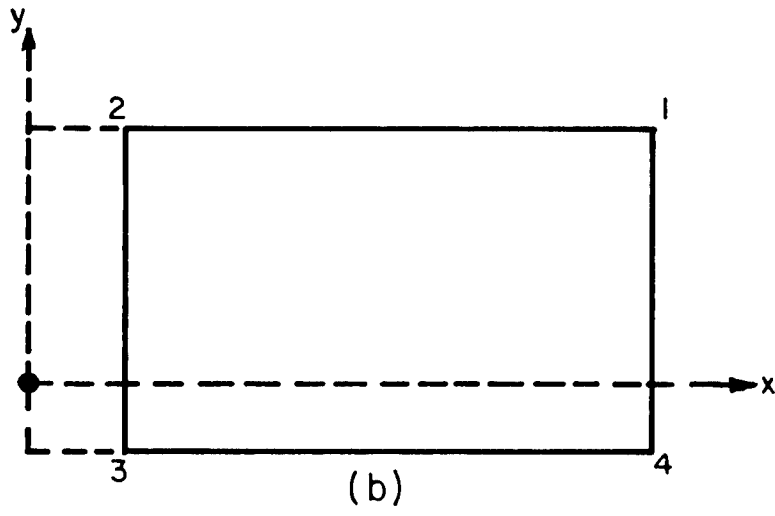
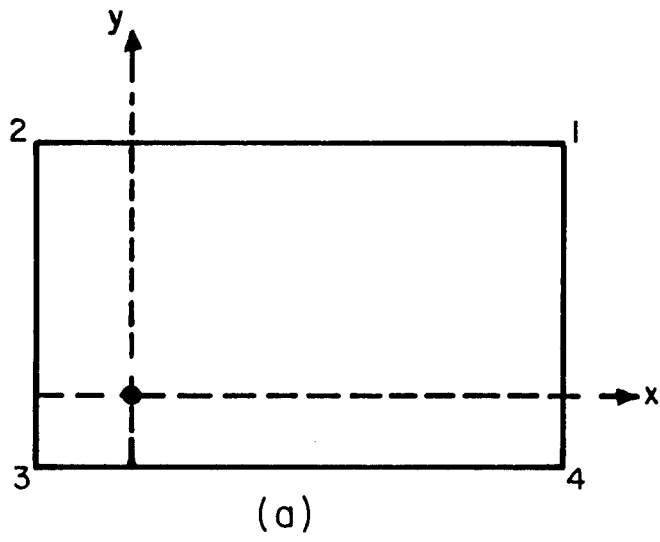


Figure 3

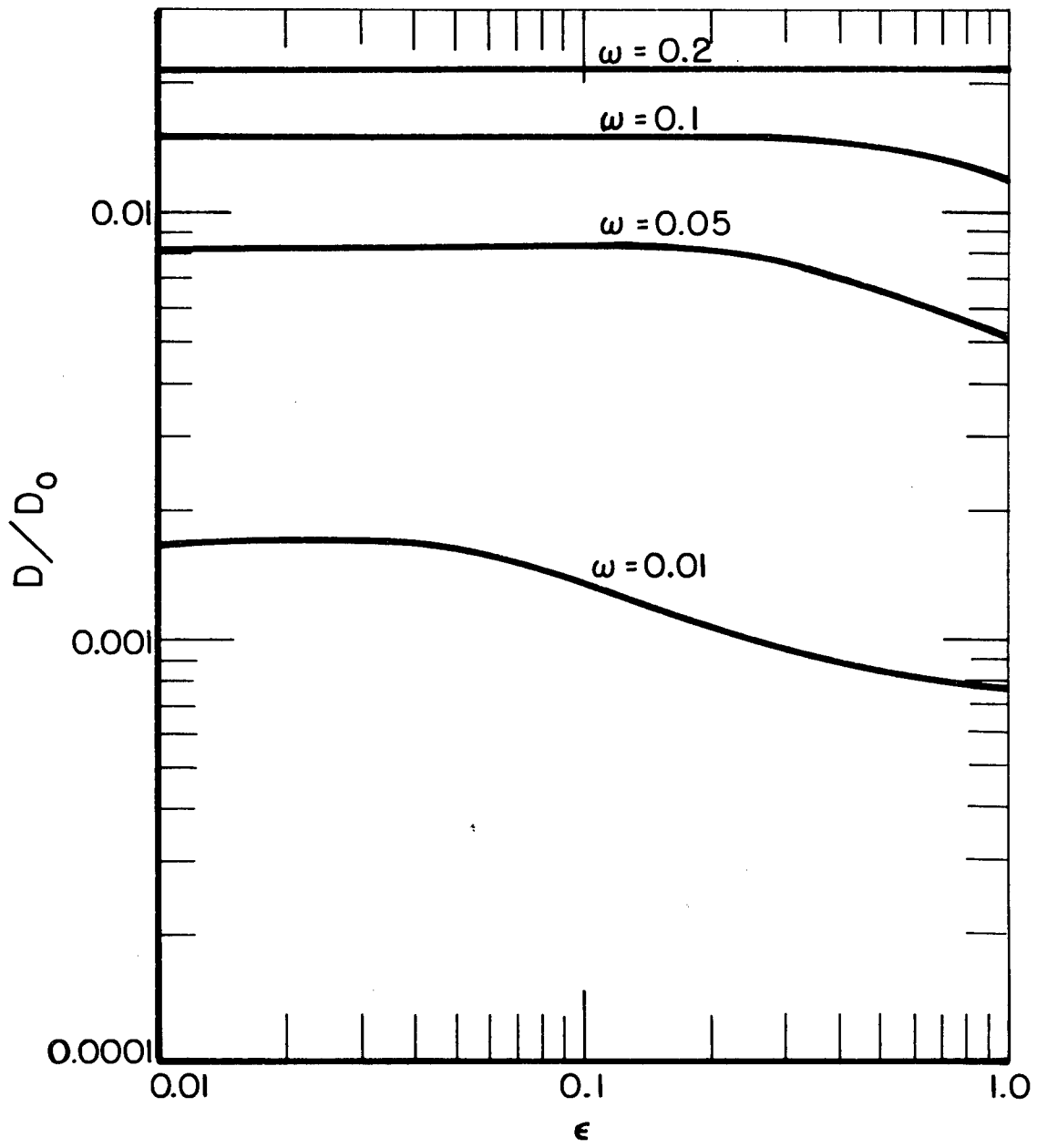


Figure 4

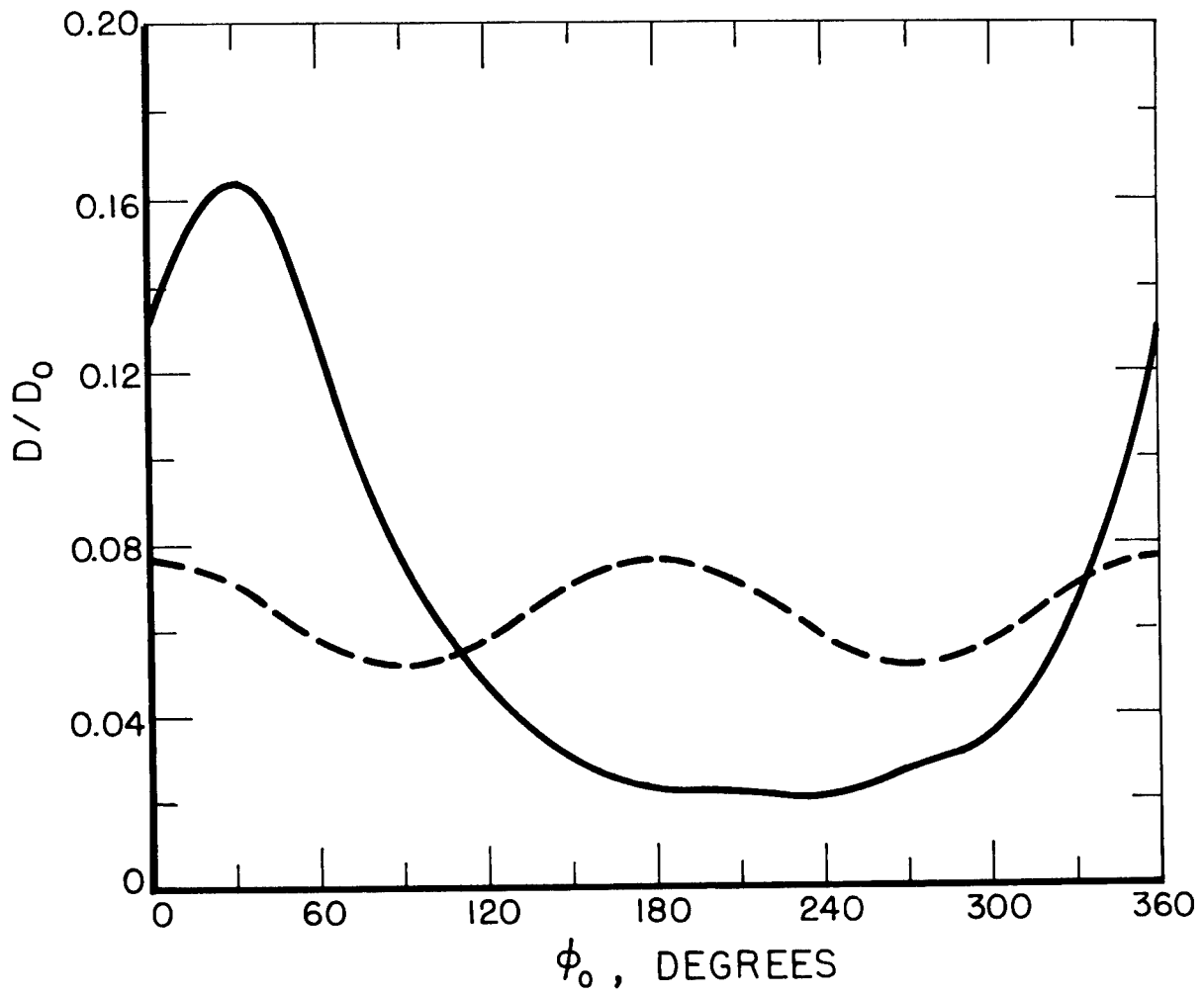


Figure 5

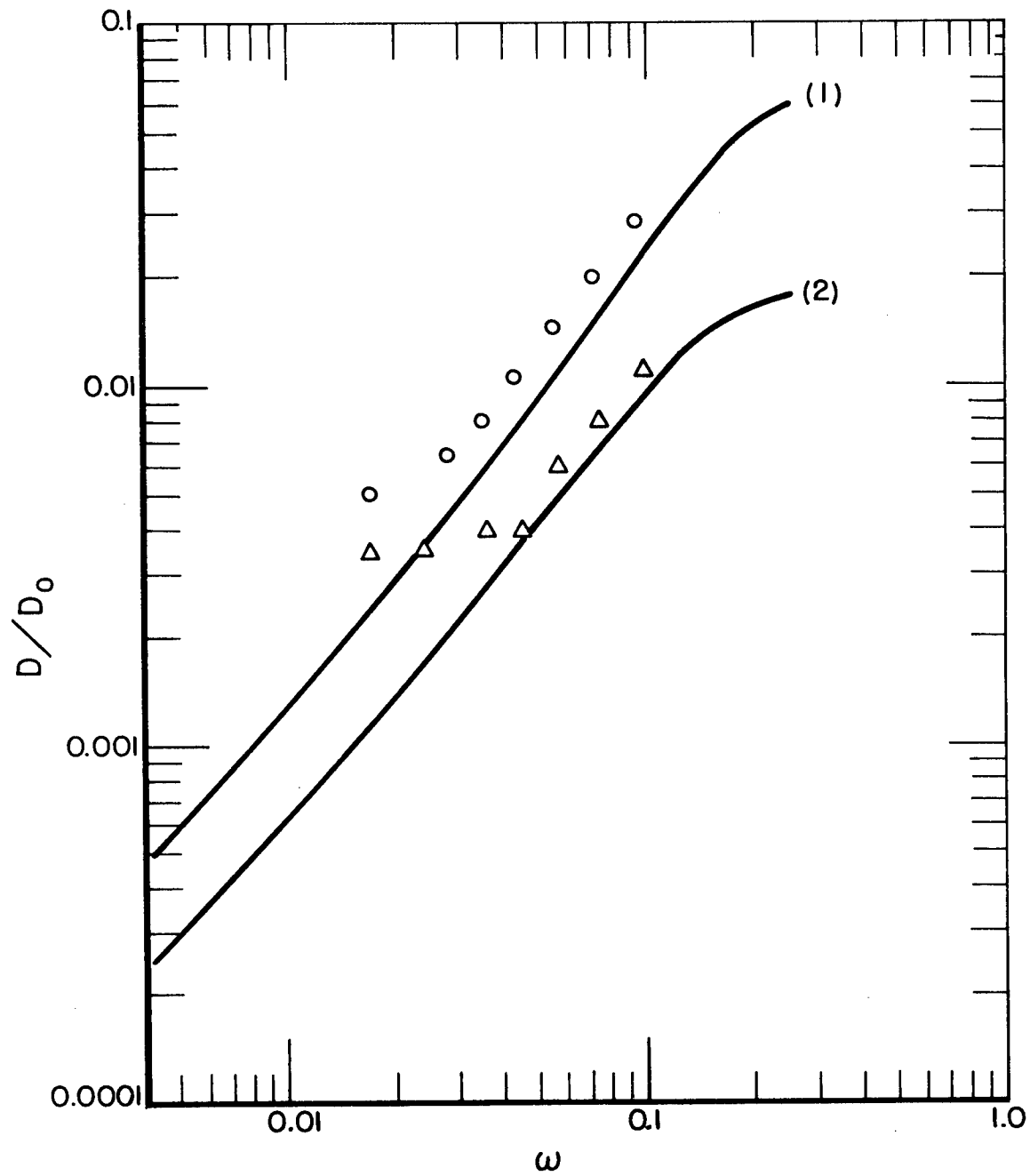


Figure 6

Table 1

Percent deviation of results using (12) and (10) from results obtained by direct numerical integration. A negative percent deviation indicates that results using (12) and (10) were smaller than results obtained by numerical integration. The values given are for a rectangle 1.0 mfp thick with eccentricity 0.5 and for radiation incident with  $\cos\theta_0 = 0.5$ .

$\varphi_0$ (degree)	$\omega$	0.2	0.1	0.02
-150		2.7	11.0	14.0
-120		1.1	1.8	12.0
-90		7.6	11.0	10.0
-60		-1.7	2.7	3.1
-30		0.9	2.4	-3.1
0		-0.8	1.5	-5.7
30		0.6	0.6	-6.7
60		0.6	1.9	-6.6
90		-1.8	-0.5	-3.5
120		1.3	5.6	3.2
150		-2.4	2.6	8.0
180		6.2	6.6	12.0

Table A1. Geometry Coefficients

EPSILON=1.000

		$G_{lm}^e$					$G_{lm}^o$				
$l$	$m$	0	1	2	3	4	0	1	2	3	4
OMEGA=0.250											
0	0	1.571E 00	7.854E-01	5.236E-01	3.927E-01	3.142E-01	6.667E-01	4.000E-01	2.857E-01	2.222E-01	1.818E-01
1	1	6.667E-01	4.000E-01	2.857E-01	2.222E-01	1.818E-01	5.000E-01	3.333E-01	2.500E-01	2.000E-01	1.667E-01
2	2	4.222E-08	2.815E-08	2.111E-08	1.689E-08	1.407E-08	1.333E-01	9.524E-02	7.407E-02	6.061E-02	5.128E-02
3	-1	1.333E-01	-9.524E-02	-7.407E-02	-6.061E-02	-5.128E-02	8.610E-08	6.457E-08	5.166E-08	4.305E-08	3.690E-08
4	-1	1.828E-08	-1.371E-08	-1.097E-08	-9.140E-09	-7.834E-09					
OMEGA=0.200											
0	0	1.257E 00	5.029E-01	2.685E-01	1.614E-01	1.035E-01	4.786E-01	2.304E-01	1.321E-01	8.253E-02	5.426E-02
1	1	4.786E-01	2.304E-01	1.321E-01	8.253E-02	5.426E-02	3.268E-01	1.762E-01	1.070E-01	6.931E-02	4.680E-02
2	2	2.111E-08	1.242E-08	5.588E-09	3.974E-09	1.656E-09	8.411E-02	4.951E-02	3.223E-02	2.188E-02	1.536E-02
3	-8	4.11E-02	-4.991E-02	-3.223E-02	-2.188E-02	-1.536E-02	3.808E-08	2.235E-08	1.391E-08	7.658E-09	4.967E-09
4	-1	3.02E-02	-1.047E-02	-8.420E-03	-6.775E-03	-5.453E-03					
OMEGA=0.150											
0	0	9.425E-01	2.836E-01	1.142E-01	5.186E-02	2.521E-02	3.124E-01	1.135E-01	4.927E-02	2.336E-02	1.169E-02
1	1	3.124E-01	1.135E-01	4.927E-02	2.336E-02	1.169E-02	1.893E-01	7.795E-02	3.622E-02	1.800E-02	9.342E-03
2	1	2.42E-08	3.725E-09	4.657E-10	-5.588E-10	-6.468E-10	4.628E-02	2.134E-02	1.090E-02	5.793E-03	3.181E-03
3	-4	6.28E-02	-2.154E-02	-1.090E-02	-5.793E-03	-3.181E-03	1.200E-08	4.191E-09	4.967E-10	-6.209E-10	-9.313E-10
4	-1	3.10E-02	-7.977E-03	-4.866E-03	-2.973E-03	-1.820E-03					
OMEGA=0.100											
0	0	6.283E-01	1.268E-01	3.448E-02	1.065E-02	3.545E-03	1.713E-01	4.205E-02	1.241E-02	4.026E-03	1.388E-03
1	1	1.713E-01	4.205E-02	1.241E-02	4.026E-03	1.388E-03	8.750E-02	2.471E-02	7.912E-03	2.724E-03	9.845E-04
2	2	4.84E-09	-1.449E-09	-1.358E-09	-9.080E-10	-5.627E-10	1.939E-02	6.342E-03	2.252E-03	8.404E-04	3.242E-04
3	-1	9.39E-02	-6.342E-03	-2.252E-03	-8.404E-04	-3.242E-04	-4.139E-10	-1.824E-09	-1.482E-09	-9.701E-10	-5.765E-10
4	-6	8.98E-03	-2.849E-03	-1.183E-03	-4.942E-04	-2.076E-04					
OMEGA=0.050											
0	0	3.142E-01	3.212E-02	4.483E-03	7.210E-04	1.266E-04	6.125E-02	7.697E-03	1.178E-03	2.010E-04	3.686E-05
1	1	6.125E-02	7.697E-03	1.178E-03	2.010E-04	3.686E-05	2.304E-02	3.394E-03	5.730E-04	1.050E-04	2.037E-05
2	-2	4.84E-09	-1.112E-09	-4.332E-10	-1.431E-10	-4.598E-11	4.044E-03	7.040E-04	1.334E-04	2.663E-05	5.520E-06
3	-4	0.44E-03	-7.040E-04	-1.334E-04	-2.663E-05	-5.520E-06	-1.811E-09	-7.567E-10	-2.648E-10	-8.721E-11	-2.764E-11
4	-1	3.67E-03	-2.912E-04	-6.282E-05	-1.373E-05	-3.038E-06					

OMEGA=0.020

0 1.257E-01 5.205E-03 2.582E-04 1.995E-05 1.475E-06  
 1 1.564E-02 8.033E-04 5.093E-05 1.564E-02 8.033E-04 5.093E-05 3.640E-06 2.827E-07  
 2 -9.507E-10 -1.738E-10 -2.660E-11 -3.786E-12 -5.197E-13 3.832E-03 2.339E-04 1.652E-05 1.278E-06 1.053E-07  
 3 -4.571E-04 -3.329E-05 -2.649E-06 -2.232E-07 -1.960E-08 4.571E-04 3.329E-05 2.649E-06 2.232E-07 1.960E-08  
 4 -1.125E-04 -9.852E-06 -8.807E-07 -8.028E-08 -7.457E-09 -3.088E-10 -4.942E-11 -7.242E-12 -1.011E-12 -1.364E-13

OMEGA=0.010

0 6.283E-02 1.308E-03 3.789E-05 1.288E-06 4.863E-08  
 1 5.547E-03 1.438E-04 4.624E-06 1.684E-07 6.690E-09 5.547E-03 1.438E-04 4.624E-06 1.684E-07 6.690E-09  
 2 -2.862E-10 -2.799E-11 -2.205E-12 -1.629E-13 -1.151E-14 9.720E-04 3.0C8E-05 1.081E-06 4.269E-08 1.802E-09  
 3 -8.402E-05 -3.112E-06 -1.261E-07 -5.422E-09 -2.434E-10 8.402E-05 3.112E-06 1.261E-07 5.422E-09 2.434E-10  
 4 -1.525E-05 -6.758E-07 -3.064E-08 -1.421E-09 -6.729E-11 -5.164E-11 -4.230E-12 -3.157E-13 -2.253E-14 -1.560E-15

OMEGA=0.005

0 3.142E-02 3.280E-04 4.778E-06 8.195E-08 1.564E-09  
 1 1.965E-03 2.559E-05 4.146E-07 7.630E-09 1.534E-10 1.965E-03 2.559E-05 4.146E-07 7.630E-09 1.534E-10  
 2 -1.067E-10 -4.383E-12 -1.662E-13 -6.090E-15 -2.161E-16 2.448E-04 3.816E-06 6.925E-08 1.382E-09 2.954E-11  
 3 -1.515E-05 -2.830E-07 -5.793E-09 -1.259E-10 -2.859E-12 1.515E-05 2.830E-07 5.793E-09 1.259E-10 2.859E-12  
 4 -1.985E-06 -4.426E-08 -1.011E-09 -2.366E-11 -5.663E-13 -7.693E-12 -3.109E-13 -1.169E-14 -4.215E-16 -1.477E-17

Table A2. Geometry Coefficients

EPSILCN=0.700

m	$G_{lm}^e$				$G_{lm}^c$					
	0	1	2	3	4	0	1	2	3	4
0	1.571E 00	7.854E-01	5.236E-01	3.927E-01	3.142E-01	6.667E-01	4.000E-01	2.857E-01	2.222E-01	1.818E-01
1	6.667E-01	4.000E-01	2.857E-01	2.222E-01	1.818E-01	5.000E-01	3.333E-01	2.500E-01	2.000E-01	1.667E-01
2	8.196E-08	5.464E-08	4.098E-08	3.278E-08	2.732E-08	1.333E-01	9.524E-02	7.407E-02	6.061E-02	5.128E-02
3	-1.333E-01	-9.524E-02	-7.407E-02	-6.061E-02	-5.128E-02	8.278E-08	6.209E-08	4.967E-08	4.139E-08	3.548E-08
4	-4.305E-08	-3.229E-08	-2.583E-08	-2.152E-08	-1.845E-08					
OMEGA=0.250										
0	1.257E 00	5.036E-01	2.696E-01	1.626E-01	1.049E-01	4.658E-01	2.206E-01	1.246E-01	7.683E-02	4.992E-02
1	4.912E-01	2.407E-01	1.406E-01	8.949E-02	5.998E-02	3.256E-01	1.756E-01	1.067E-01	6.924E-02	4.688E-02
2	2.716E-02	2.154E-02	1.710E-02	1.359E-02	1.080E-02	1.016E-01	6.385E-02	4.333E-02	3.074E-02	2.243E-02
3	-6.314E-02	-3.324E-02	-1.897E-02	-1.133E-02	-6.954E-03	2.086E-02	1.668E-02	1.335E-02	1.069E-02	8.570E-03
4	-9.510E-03	-7.517E-03	-5.950E-03	-4.716E-03	-3.743E-03					
OMEGA=0.150										
0	9.425E-01	2.856E-01	1.165E-01	5.392E-02	2.684E-02	2.938E-01	1.035E-01	4.392E-02	2.051E-02	1.019E-02
1	3.316E-01	1.257E-01	5.699E-02	2.826E-02	1.480E-02	1.882E-01	7.750E-02	3.654E-02	1.841E-02	9.720E-03
2	3.481E-02	2.055E-02	1.218E-02	7.251E-03	4.336E-03	6.563E-02	3.310E-02	1.784E-02	9.991E-03	5.734E-03
3	-2.274E-02	-7.585E-03	-2.599E-03	-8.433E-04	-2.211E-04	2.052E-02	1.237E-02	7.487E-03	4.551E-03	2.777E-03
4	-8.937E-03	-5.282E-03	-3.147E-03	-1.890E-03	-1.144E-03					
OMEGA=0.100										
0	6.283E-01	1.293E-01	3.637E-02	1.176E-02	4.132E-03	1.550E-01	3.663E-02	1.064E-02	3.467E-03	1.219E-03
1	1.890E-01	4.983E-02	1.582E-02	5.527E-03	2.048E-03	8.698E-02	2.459E-02	8.232E-03	2.938E-03	1.107E-03
2	2.561E-02	1.004E-02	3.986E-03	1.602E-03	6.513E-04	3.099E-02	1.102E-02	4.172E-03	1.641E-03	6.630E-04
3	-4.981E-03	-6.560E-04	8.522E-06	6.528E-05	4.116E-05	1.046E-02	4.271E-03	1.764E-03	7.364E-04	3.106E-04
4	-4.378E-03	-1.763E-03	-7.263E-04	-3.056E-04	-1.310E-04					
OMEGA=0.050										
0	3.142E-01	3.337E-02	4.966E-03	8.639E-04	1.651E-04	5.320E-02	6.481E-03	1.003E-03	1.785E-04	3.480E-05
1	7.039E-02	9.795E-03	1.660E-03	3.121E-04	6.264E-05	2.955E-02	3.511E-03	6.253E-04	1.220E-04	2.531E-05
2	9.162E-03	1.805E-03	3.652E-04	7.578E-05	1.610E-05	6.995E-03	1.319E-03	2.660E-04	5.616E-05	1.227E-05
3	-3.036E-04	3.743E-05	1.603E-05	3.934E-06	8.210E-07	1.984E-03	4.182E-04	9.028E-05	1.991E-05	4.480E-06
4	-8.253E-04	-1.769E-04	-3.957E-05	-9.160E-06	-2.179E-06					



Table A3. Geometry Coefficients

m	$G_{lm}^e$					$G_{lm}^o$				
	0	1	2	3	4	0	1	2	3	4
EPSILON=0.500										
OMEGA=0.250										
0	1.571E 00	7.854E-01	5.236E-01	3.927E-01	3.142E-01	6.667E-01	4.000E-01	2.857E-01	2.222E-01	1.818E-01
1	6.667E-01	4.000E-01	2.857E-01	2.222E-01	1.818E-01	5.000E-01	3.333E-01	2.500E-01	2.000E-01	1.667E-01
2	6.954E-08	4.636E-08	3.477E-08	2.782E-08	2.318E-08	1.333E-01	9.524E-02	7.407E-02	6.061E-02	5.128E-02
3	-1.333E-01	-9.524E-02	-7.407E-02	-6.061E-02	-5.128E-02	-1.656E-09	-1.242E-09	-9.934E-10	-8.278E-10	-7.096E-10
4	-4.553E-08	-3.415E-08	-2.732E-08	-2.277E-08	-1.951E-08					
OMEGA=0.200										
0	1.257E 00	5.051E-01	2.719E-01	1.654E-01	1.078E-01	4.557E-01	2.133E-01	1.193E-01	7.301E-02	4.720E-02
1	5.009E-01	2.493E-01	1.482E-01	9.612E-02	6.577E-02	3.232E-01	1.741E-01	1.060E-01	6.901E-02	4.697E-02
2	4.816E-02	3.849E-02	3.084E-02	2.475E-02	2.009E-02	1.124E-01	7.256E-02	5.043E-02	3.655E-02	2.720E-02
3	-4.479E-02	-1.840E-02	-6.940E-03	-1.553E-03	1.009E-03	3.568E-02	2.870E-02	2.313E-02	1.868E-02	1.511E-02
4	-1.915E-03	-1.016E-03	-4.089E-04	-9.193E-06	2.437E-04					
OMEGA=0.150										
0	9.425E-01	2.901E-01	1.219E-01	5.888E-02	3.089E-02	2.791E-01	9.656E-02	4.077E-02	1.921E-02	9.748E-03
1	3.474E-01	1.376E-01	6.569E-02	3.452E-02	1.925E-02	1.856E-01	7.764E-02	3.719E-02	1.930E-02	1.059E-02
2	6.321E-02	3.822E-02	2.337E-02	1.445E-02	9.019E-03	7.800E-02	4.099E-02	2.298E-02	1.340E-02	8.025E-03
3	-5.672E-04	6.231E-03	6.117E-03	4.717E-03	3.361E-03	3.602E-02	2.219E-02	1.381E-02	8.670E-03	5.492E-03
4	7.448E-04	1.270E-03	1.249E-03	1.044E-03	8.080E-04					
OMEGA=0.100										
0	6.283E-01	1.353E-01	4.126E-02	1.481E-02	5.854E-03	1.419E-01	3.329E-02	9.591E-03	3.475E-03	1.336E-03
1	2.052E-01	5.906E-02	2.081E-02	8.149E-03	3.405E-03	8.559E-02	2.563E-02	9.015E-03	3.496E-03	1.448E-03
2	4.822E-02	1.957E-02	8.523E-03	3.735E-03	1.674E-03	3.892E-02	1.475E-02	6.001E-03	2.559E-03	1.130E-03
3	1.011E-02	5.944E-03	2.579E-03	1.434E-03	6.830E-04	1.915E-02	8.249E-03	3.643E-03	1.644E-03	7.565E-04
4	2.093E-03	1.250E-03	7.067E-04	3.669E-04	1.853E-04					
OMEGA=0.050										
0	3.142E-01	3.672E-02	6.367E-03	1.323E-03	3.036E-04	4.673E-02	5.886E-03	1.014E-03	2.090E-04	4.795E-05
1	7.973E-02	1.284E-02	2.573E-03	5.769E-04	1.383E-04	2.268E-02	3.815E-03	7.739E-04	1.751E-04	4.243E-05
2	1.804E-02	3.936E-03	9.090E-04	2.196E-04	5.495E-05	9.207E-03	1.928E-03	4.402E-04	1.066E-04	2.695E-05
3	4.134E-03	1.085E-03	2.751E-04	7.016E-05	1.814E-05	3.843E-03	8.977E-04	2.193E-04	5.550E-05	1.445E-05
4	7.399E-04	2.104E-04	5.688E-05	1.508E-05	3.974E-06					

OMEGA=0.020

0 1.257E-01 6.270E-03 4.761E-04 4.349E-05 4.382E-06  
 1 2.141E-02 1.488E-03 1.299E-04 1.271E-05 1.330E-06  
 2 3.516E-03 3.206E-04 3.147E-05 3.265E-06 3.530E-07  
 3 5.835E-04 6.144E-05 6.482E-06 6.989E-07 7.710E-08  
 4 7.265E-05 8.173E-06 8.946E-07 9.727E-08 1.058E-08

OMEGA=0.010

0 6.283E-02 1.605E-03 6.288E-05 2.964E-06 1.541E-07  
 1 7.721E-03 2.756E-04 1.238E-04 6.233E-07 3.361E-08  
 2 9.328E-04 4.322E-05 2.168E-06 1.153E-07 6.406E-09  
 3 1.134E-04 6.005E-06 3.218E-07 1.770E-08 9.993E-10  
 4 1.022E-05 5.740E-07 3.156E-08 1.729E-09 9.486E-11

OMEGA=0.005

0 3.142E-02 4.062E-04 8.082E-06 1.935E-07 5.109E-09  
 1 2.757E-03 4.985E-05 1.136E-06 2.903E-08 7.943E-10  
 2 2.400E-04 5.606E-06 1.422E-07 3.831E-09 1.079E-10  
 3 2.095E-05 5.571E-07 1.505E-08 4.183E-10 1.194E-11  
 4 1.349E-06 3.787E-08 1.043E-09 2.867E-11 7.893E-13

4.749E-05 4.398E-06 4.516E-07  
 2.512E-05 2.519E-06 2.702E-07  
 9.847E-06 1.044E-06 1.158E-07  
 3.334E-06 3.668E-07 4.169E-08  
 6.169E-04 1.138E-02 1.138E-02  
 2.798E-04 3.804E-03 3.804E-03  
 9.910E-05 1.100E-03 1.100E-03  
 3.161E-05 3.170E-04 3.170E-04  
 1.110E-04 3.978E-03 3.978E-03  
 3.678E-05 9.683E-04 9.683E-04  
 9.455E-06 2.052E-04 2.052E-04  
 2.194E-06 4.296E-05 4.296E-05  
 4.446E-06 2.142E-07 2.142E-07  
 1.710E-06 8.878E-08 8.878E-08  
 4.861E-07 2.659E-08 2.659E-08  
 1.189E-07 6.739E-09 6.739E-09

4.051E-07 9.952E-09 2.701E-10  
 1.116E-07 2.950E-09 8.333E-11  
 2.272E-08 6.314E-10 1.838E-11  
 3.972E-09 1.142E-10 3.401E-12  
 1.983E-05 4.718E-06 4.718E-06  
 8.740E-07 2.272E-08 2.272E-08  
 1.445E-07 3.972E-09 3.972E-09

Table A4. Geometry Coefficients

EPSILCN=0.333

		$G_{lm}^c$				$G_{lm}^s$					
		0	1	2	3	4	0	1	2	3	4
OMEGA=0.250											
0	1.571E 00	7.854E-01	5.236E-01	3.927E-01	3.142E-01	3.142E-01	6.667E-01	4.060E-01	2.857E-01	2.222E-01	1.818E-01
1	6.667E-01	4.060E-01	2.857E-01	2.222E-01	1.818E-01	1.818E-01	5.000E-01	3.333E-01	2.500E-01	2.000E-01	1.667E-01
2	7.202E-08	4.801E-08	3.601E-08	2.881E-08	2.401E-08	2.401E-08	1.333E-01	9.524E-02	7.407E-02	6.061E-02	5.128E-02
3	-1.333E-01	-9.524E-02	-7.407E-02	-6.061E-02	-5.128E-02	-5.128E-02	-1.325E-08	-9.934E-09	-7.947E-09	-6.623E-09	-5.677E-09
4	-6.871E-08	-5.153E-08	-4.123E-08	-3.436E-08	-2.945E-08	-2.945E-08					
OMEGA=0.200											
0	1.257E 00	5.069E-01	2.749E-01	1.691E-01	1.118E-01	1.118E-01	4.473E-01	2.073E-01	1.151E-01	7.010E-02	4.522E-02
1	5.087E-01	2.568E-01	1.552E-01	1.026E-01	7.177E-02	7.177E-02	3.199E-01	1.721E-01	1.048E-01	6.850E-02	4.690E-02
2	6.515E-02	5.262E-02	4.267E-02	3.474E-02	2.839E-02	2.839E-02	1.188E-01	7.751E-02	5.494E-02	4.038E-02	3.050E-02
3	-2.860E-02	-4.935E-03	4.330E-03	7.931E-03	9.033E-03	9.033E-03	4.585E-02	3.712E-02	3.016E-02	2.458E-02	2.011E-02
4	7.500E-03	7.281E-03	6.881E-03	6.382E-03	5.839E-03	5.839E-03					
OMEGA=0.150											
0	9.425E-01	2.963E-01	1.297E-01	6.632E-02	3.730E-02	3.730E-02	2.664E-01	9.099E-02	3.856E-02	1.855E-02	9.761E-03
1	3.616E-01	1.459E-01	7.586E-02	4.265E-02	2.562E-02	2.562E-02	1.819E-01	7.656E-02	3.780E-02	2.038E-02	1.173E-02
2	8.831E-02	5.526E-02	3.530E-02	2.300E-02	1.525E-02	1.525E-02	8.590E-02	4.659E-02	2.711E-02	1.651E-02	1.040E-02
3	2.128E-02	2.104E-02	1.640E-02	1.200E-02	8.603E-03	8.603E-03	4.768E-02	3.020E-02	1.947E-02	1.276E-02	8.498E-03
4	1.429E-02	1.116E-02	8.456E-03	6.306E-03	4.659E-03	4.659E-03					
OMEGA=0.100											
0	6.283E-01	1.448E-01	4.963E-02	2.059E-02	9.528E-03	9.528E-03	1.299E-01	3.078E-02	9.861E-03	3.816E-03	1.672E-03
1	2.219E-01	7.108E-02	2.860E-02	1.297E-02	6.326E-03	6.326E-03	8.328E-02	2.641E-02	1.019E-02	4.438E-03	2.095E-03
2	7.131E-02	3.213E-02	1.529E-02	7.610E-03	3.924E-03	3.924E-03	4.472E-02	1.826E-02	8.177E-03	3.903E-03	1.954E-03
3	2.789E-02	1.520E-02	8.024E-03	4.265E-03	2.300E-03	2.300E-03	2.692E-02	1.253E-02	6.105E-03	3.088E-03	1.610E-03
4	1.301E-02	7.252E-03	4.049E-03	2.252E-03	1.259E-03	1.259E-03					
OMEGA=0.050											
0	3.142E-01	4.310E-02	9.455E-03	2.536E-03	7.535E-04	7.535E-04	4.043E-02	5.585E-03	1.169E-03	3.041E-04	8.885E-05
1	9.127E-02	1.805E-02	4.590E-03	1.320E-03	4.075E-04	4.075E-04	2.215E-02	4.349E-03	1.083E-03	3.073E-04	9.410E-05
2	2.908E-02	7.544E-03	2.155E-03	6.576E-04	2.102E-04	2.102E-04	1.124E-02	2.771E-03	7.720E-04	2.326E-04	7.387E-05
3	1.078E-02	3.151E-03	5.810E-04	3.132E-04	1.031E-04	1.031E-04	5.984E-03	1.658E-03	4.949E-04	1.557E-04	5.086E-05
4	4.146E-03	1.314E-03	4.252E-04	1.407E-04	4.748E-05	4.748E-05					



Table A5. Geometry Coefficients

EPSILON=0.200

m	$C_{lm}^e$					$C_{lm}^o$				
	0	1	2	3	4	0	1	2	3	4
0	1.571E-00	7.854E-01	5.236E-01	3.927E-01	3.142E-01	6.667E-01	4.000E-01	2.857E-01	2.222E-01	1.818E-01
1	6.667E-01	4.000E-01	2.857E-01	2.222E-01	1.818E-01	5.000E-01	3.333E-01	2.500E-01	2.000E-01	1.667E-01
2	6.830E-08	4.553E-08	3.415E-08	2.732E-08	2.277E-08	1.333E-01	9.524E-02	7.407E-02	6.061E-02	5.128E-02
3	-1.333E-01	-9.524E-02	-7.407E-02	-6.061E-02	-5.128E-02	5.691E-08	-4.249E-08	-3.415E-08	-2.846E-08	-2.439E-08
4	-7.782E-08	-5.836E-08	-4.669E-08	-3.891E-08	-3.335E-08	5.082E-02	4.130E-02	3.373E-02	2.768E-02	2.282E-02
0	1.257E-00	5.084E-01	2.775E-01	1.723E-01	1.154E-01	4.418E-01	2.034E-01	1.124E-01	6.820E-02	4.393E-02
1	5.137E-01	2.619E-01	1.603E-01	1.076E-01	7.659E-02	3.170E-01	1.702E-01	1.036E-01	6.782E-02	4.659E-02
2	7.604E-02	6.200E-02	5.084E-02	4.194E-02	3.478E-02	1.215E-01	8.018E-02	5.691E-02	4.214E-02	3.208E-02
3	-1.759E-02	4.552E-03	1.258E-02	1.516E-02	1.542E-02	5.082E-02	4.130E-02	3.373E-02	2.768E-02	2.282E-02
4	1.520E-02	1.431E-02	1.328E-02	1.221E-02	1.114E-02	5.386E-02	3.484E-02	2.313E-02	1.573E-02	1.094E-02
0	9.425E-01	3.021E-01	1.373E-01	7.399E-02	4.436E-02	2.576E-01	8.717E-02	3.708E-02	1.816E-02	9.866E-03
1	3.716E-01	1.599E-01	8.506E-02	5.075E-02	3.260E-02	1.782E-01	7.588E-02	3.796E-02	2.108E-02	1.262E-02
2	1.061E-01	6.862E-02	4.576E-02	3.139E-02	2.208E-02	8.926E-02	4.935E-02	2.948E-02	1.857E-02	1.218E-02
3	3.815E-02	3.366E-02	2.617E-02	1.974E-02	1.482E-02	5.386E-02	3.484E-02	2.313E-02	1.573E-02	1.094E-02
4	2.706E-02	2.135E-02	1.663E-02	1.290E-02	1.000E-02	5.386E-02	3.484E-02	2.313E-02	1.573E-02	1.094E-02
0	6.283E-01	1.553E-01	6.001E-02	2.876E-02	1.553E-02	1.207E-01	2.897E-02	9.918E-03	4.260E-03	2.117E-03
1	2.361E-01	8.376E-02	3.838E-02	2.012E-02	1.143E-02	8.045E-02	2.683E-02	1.128E-02	5.491E-03	2.941E-03
2	9.116E-02	4.504E-02	2.411E-02	1.374E-02	8.201E-03	4.763E-02	2.078E-02	1.020E-02	5.442E-03	3.088E-03
3	4.520E-02	2.624E-02	1.541E-02	9.313E-03	5.786E-03	3.203E-02	1.609E-02	8.644E-03	4.904E-03	2.905E-03
4	2.624E-02	1.603E-02	9.933E-03	6.266E-03	4.022E-03	3.480E-02	5.472E-03	1.453E-03	4.951E-04	1.911E-04
0	3.142E-01	5.284E-02	1.532E-02	5.512E-03	2.202E-03	2.126E-02	5.036E-03	1.602E-03	5.930E-04	2.395E-04
1	1.044E-01	2.631E-02	8.839E-03	3.397E-03	1.408E-03	1.281E-02	3.866E-03	1.375E-03	5.401E-04	2.260E-04
2	4.236E-02	1.379E-02	5.138E-03	2.082E-03	8.902E-04	8.177E-03	2.811E-03	1.076E-03	4.414E-04	1.901E-04
3	2.039E-02	7.528E-03	3.004E-03	1.268E-03	5.569E-04	8.177E-03	2.811E-03	1.076E-03	4.414E-04	1.901E-04
4	1.052E-02	4.190E-03	1.757E-03	7.666E-04	3.444E-04	8.177E-03	2.811E-03	1.076E-03	4.414E-04	1.901E-04

OMEGA=0.250

OMEGA=0.200

OMEGA=0.150

OMEGA=0.100

OMEGA=0.050



Table A6. Geometry Coefficients

EPSILON=0.100

m	$C_{lm}^e$					$C_{lm}^o$				
	0	1	2	3	4	0	1	2	3	4
OMEGA=0.250										
0	1.571E 00	7.854E-01	5.236E-01	3.927E-01	3.142E-01					
1	6.667E-01	4.0C0E-01	2.857E-01	2.222E-01	1.818E-01	6.667E-01	4.0C0E-01	2.857E-01	2.222E-01	1.818E-01
2	3.601E-08	2.401E-08	1.801E-08	1.440E-08	1.200E-08	5.000E-01	3.333E-01	2.500E-01	2.000E-01	1.667E-01
3	-1.333E-01	-9.524E-02	-7.407E-02	-6.061E-02	-5.128E-02	1.333E-01	9.524E-02	7.407E-02	6.061E-02	5.128E-02
4	1.991E-07	1.493E-07	1.195E-07	9.955E-08	8.533E-08	-4.139E-09	-3.104E-09	-2.484E-09	-2.070E-09	-1.774E-09
OMEGA=0.200										
0	1.257E 00	5.093E-01	2.790E-01	1.742E-01	1.176E-01					
1	5.161E-01	2.645E-01	1.630E-01	1.104E-01	7.938E-02	4.390E-01	2.014E-01	1.110E-01	6.721E-02	4.324E-02
2	8.131E-02	6.669E-02	5.508E-02	4.582E-02	3.837E-02	3.153E-01	1.690E-01	1.028E-01	6.726E-02	4.625E-02
3	-1.206E-02	9.472E-03	1.701E-02	1.920E-02	1.913E-02	1.221E-01	8.073E-02	5.740E-02	4.259E-02	3.251E-02
4	1.946E-02	1.823E-02	1.707E-02	1.578E-02	1.450E-02	5.244E-02	4.266E-02	3.489E-02	2.869E-02	2.373E-02
OMEGA=0.150										
0	9.425E-01	3.056E-01	1.422E-01	7.928E-02	4.955E-02					
1	3.768E-01	1.658E-01	9.093E-02	5.636E-02	3.783E-02	2.530E-01	8.510E-02	3.622E-02	1.788E-02	9.857E-03
2	1.155E-01	7.634E-02	5.242E-02	3.726E-02	2.731E-02	1.757E-01	7.488E-02	3.773E-02	2.122E-02	1.295E-02
3	4.757E-02	4.138E-02	3.275E-02	2.547E-02	1.987E-02	8.992E-02	5.0C3E-02	3.022E-02	1.934E-02	1.295E-02
4	3.505E-02	2.829E-02	2.270E-02	1.824E-02	1.473E-02	5.584E-02	3.643E-02	2.451E-02	1.698E-02	1.208E-02
OMEGA=0.100										
0	6.283E-01	1.630E-01	6.855E-02	3.642E-02	2.202E-02					
1	2.448E-01	9.314E-02	4.679E-02	2.726E-02	1.736E-02	1.154E-01	2.781E-02	9.870E-03	4.503E-03	2.414E-03
2	1.038E-01	5.492E-02	3.216E-02	2.032E-02	1.359E-02	7.810E-02	2.668E-02	1.177E-02	6.120E-03	3.547E-03
3	5.730E-02	3.551E-02	2.280E-02	1.528E-02	1.063E-02	4.817E-02	2.176E-02	1.127E-02	6.445E-03	3.969E-03
4	3.687E-02	2.433E-02	1.656E-02	1.159E-02	8.329E-03	3.393E-02	1.780E-02	1.016E-02	6.212E-03	4.008E-03
OMEGA=0.050										
0	3.142E-01	6.379E-02	2.382E-02	1.122E-02	5.913E-03					
1	1.161E-01	3.634E-02	1.587E-02	8.004E-03	4.386E-03	3.068E-02	5.356E-03	1.730E-03	7.399E-04	3.648E-04
2	5.550E-02	2.255E-02	1.086E-02	5.775E-03	3.268E-03	2.010E-02	5.540E-03	2.166E-03	1.013E-03	5.249E-04
3	3.165E-02	1.469E-02	7.586E-03	4.206E-03	2.445E-03	1.349E-02	4.833E-03	2.132E-03	1.064E-03	5.738E-04
4	1.961E-02	9.899E-03	5.386E-03	3.086E-03	1.836E-03	9.686E-03	4.028E-03	1.930E-03	1.012E-03	5.637E-04

OMEGA=0.020

0	1.257E-01	1.711E-02	4.343E-03	1.350E-03	4.630E-04	7.354E-C4	1.749E-04	5.240E-05	1.754E-05
1	3.920E-02	8.242E-03	2.373E-03	7.811E-04	2.767E-04	5.981E-03	1.867E-04	5.972E-05	2.075E-05
2	1.634E-02	4.257E-03	1.331E-03	4.575E-04	1.664E-04	3.479E-03	1.549E-04	5.198E-05	1.861E-05
3	7.824E-03	2.297E-03	7.613E-04	2.706E-04	1.006E-04	2.094E-03	1.171E-04	4.079E-05	1.496E-05
4	4.019E-03	1.276E-03	4.414E-04	1.612E-04	6.101E-05	1.301E-03			

OMEGA=0.010

0	6.284E-02	5.327E-03	8.287E-04	1.559E-04	3.218E-05	1.920E-03	2.327E-05	4.312E-06	8.826E-07
1	1.561E-02	2.018E-03	3.529E-04	7.005E-05	1.490E-05	9.183E-04	1.961E-05	3.851E-06	8.148E-07
2	5.170E-03	8.168E-04	1.542E-04	3.186E-05	6.948E-06	4.481E-04	1.279E-05	2.622E-06	5.695E-07
3	1.946E-03	3.443E-04	6.860E-05	1.462E-05	3.254E-06	2.224E-04	7.580E-06	1.606E-06	3.566E-07
4	7.824E-04	1.491E-04	3.092E-05	6.757E-06	1.529E-06				

OMEGA=0.005

0	3.142E-02	1.491E-03	1.283E-04	1.326E-05	1.500E-06	6.489E-04	2.550E-06	2.626E-07	2.968E-08
1	5.869E-03	4.209E-04	4.053E-05	4.412E-06	5.139E-07	2.377E-04	1.605E-06	1.744E-07	2.034E-08
2	1.455E-03	1.267E-04	1.313E-05	1.486E-06	1.772E-07	8.787E-05	7.796E-07	8.822E-08	1.054E-08
3	4.081E-04	3.964E-05	4.328E-06	5.047E-07	6.137E-08	3.156E-C6	3.438E-07	4.013E-08	4.894E-09
4	1.220E-04	1.273E-05	1.445E-06	1.726E-07	2.132E-08				

Table A7. Geometry Coefficients

EPSILON=0.050

		$G_{lm}^e$					$G_{lm}^o$				
		0	1	2	3	4	0	1	2	3	4
OMEGA=0.250											
0	1.571E 00	7.854E-01	5.236E-01	3.927E-01	3.142E-01	6.667E-01	4.000E-01	2.857E-01	2.222E-01	1.818E-01	
1	6.667E-01	4.000E-01	2.857E-01	2.222E-01	1.818E-01	5.000E-01	3.333E-01	2.500E-01	2.000E-01	1.667E-01	
2	7.916E-08	5.277E-08	3.958E-08	3.166E-08	2.639E-08	1.333E-01	9.524E-02	7.407E-02	6.061E-02	5.128E-02	
3	-1.333E-01	-9.524E-02	-7.407E-02	-6.061E-02	-5.128E-02	-3.626E-08	-2.719E-08	-2.175E-08	-1.813E-08	-1.554E-08	
4	-1.343E-07	-1.007E-07	-8.059E-08	-6.716E-08	-5.756E-08						
OMEGA=0.200											
0	1.257E 00	5.056E-01	2.794E-01	1.748E-01	1.182E-01	4.383E-01	2.009E-01	1.106E-01	6.692E-02	4.303E-02	
1	5.167E-01	2.652E-01	1.638E-01	1.112E-01	8.022E-02	3.148E-01	1.686E-01	1.025E-01	6.705E-02	4.610E-02	
2	8.271E-02	6.797E-02	5.627E-02	4.693E-02	3.943E-02	1.222E-01	8.076E-02	5.742E-02	4.261E-02	3.254E-02	
3	-1.056E-02	1.083E-02	1.827E-02	2.038E-02	2.024E-02	5.221E-02	4.287E-02	3.506E-02	2.884E-02	2.386E-02	
4	2.067E-02	1.949E-02	1.819E-02	1.686E-02	1.555E-02						
OMEGA=0.150											
0	9.425E-01	3.067E-01	1.438E-01	8.103E-02	5.136E-02	2.517E-01	8.449E-02	3.594E-02	1.776E-02	9.817E-03	
1	3.783E-01	1.675E-01	9.279E-02	5.824E-02	3.967E-02	1.749E-01	7.449E-02	3.756E-02	2.117E-02	1.296E-02	
2	1.181E-01	7.865E-02	5.454E-02	3.925E-02	2.920E-02	8.986E-02	5.002E-02	3.026E-02	1.942E-02	1.306E-02	
3	5.029E-02	4.376E-02	3.491E-02	2.747E-02	2.175E-02	5.609E-02	3.663E-02	2.470E-02	1.717E-02	1.228E-02	
4	3.751E-02	3.055E-02	2.480E-02	2.020E-02	1.657E-02						
OMEGA=0.100											
0	6.283E-01	1.657E-01	7.170E-02	3.954E-02	2.494E-02	1.138E-01	2.740E-02	9.793E-03	4.530E-03	2.474E-03	
1	2.475E-01	9.639E-02	5.003E-02	3.031E-02	2.017E-02	7.721E-02	2.648E-02	1.181E-02	6.233E-03	3.687E-03	
2	1.077E-01	5.847E-02	3.540E-02	2.328E-02	1.627E-02	4.800E-02	2.182E-02	1.144E-02	6.660E-03	4.193E-03	
3	6.135E-02	3.903E-02	2.595E-02	1.812E-02	1.319E-02	3.412E-02	1.806E-02	1.047E-02	6.525E-03	4.312E-03	
4	4.071E-02	2.773E-02	1.958E-02	1.431E-02	1.077E-02						
OMEGA=0.050											
0	3.142E-01	6.905E-02	2.882E-02	1.537E-02	9.264E-03	2.916E-02	5.241E-03	1.804E-03	8.376E-04	4.545E-04	
1	1.210E-01	4.192E-02	2.048E-02	1.175E-02	7.381E-03	1.945E-02	5.614E-03	2.358E-03	1.205E-03	6.908E-04	
2	6.147E-02	2.765E-02	1.504E-02	9.127E-03	5.937E-03	1.344E-02	5.099E-03	2.435E-03	1.336E-03	8.011E-04	
3	3.741E-02	1.936E-02	1.134E-02	7.195E-03	4.818E-03	9.992E-03	4.446E-03	2.322E-03	1.346E-03	8.379E-04	
4	2.490E-02	1.411E-02	8.735E-03	5.743E-03	3.941E-03						

OMEGA=0.020

0	1.257E-01	2.264E-02	7.959E-03	3.479E-03	1.693E-03	5.089E-03	7.660E-04	2.395E-04	9.706E-05	4.481E-05
1	4.504E-02	1.285E-02	5.161E-03	2.400E-03	1.211E-03	3.269E-03	8.117E-04	2.975E-04	1.300E-04	6.273E-05
2	2.208E-02	7.887E-03	3.459E-03	1.686E-03	8.752E-04	2.226E-03	7.105E-04	2.892E-04	1.337E-04	6.686E-05
3	1.252E-02	5.089E-03	2.376E-03	1.201E-03	6.384E-04	1.584E-03	5.877E-04	2.578E-04	1.246E-04	6.413E-05
4	7.679E-03	3.400E-03	1.663E-03	8.654E-04	4.693E-04					

OMEGA=0.010

0	6.284E-02	8.407E-03	2.145E-03	6.699E-04	2.309E-04	1.496E-03	1.783E-04	4.277E-05	1.292E-05	4.376E-06
1	1.959E-02	4.085E-03	1.178E-03	3.894E-04	1.387E-04	8.691E-04	1.670E-04	4.607E-05	1.486E-05	5.228E-06
2	8.311E-03	2.135E-03	6.676E-04	2.302E-04	8.412E-05	5.280E-04	1.277E-04	3.862E-05	1.309E-05	4.743E-06
3	4.032E-03	1.169E-03	3.870E-04	1.379E-04	5.144E-05	3.304E-04	9.155E-05	2.958E-05	1.041E-05	3.864E-06
4	2.105E-03	6.608E-04	2.283E-04	8.346E-05	3.167E-05					

OMEGA=0.005

0	3.145E-02	2.653E-03	4.174E-04	7.943E-05	1.656E-05	4.804E-04	3.817E-05	5.873E-06	1.112E-06	2.326E-07
1	7.833E-03	1.015E-03	1.792E-04	3.594E-05	7.717E-06	2.302E-04	2.876E-05	5.021E-06	1.007E-06	2.173E-07
2	2.633E-03	4.160E-04	7.922E-05	1.652E-05	3.629E-06	1.136E-04	1.755E-05	3.328E-06	6.960E-07	1.538E-07
3	1.006E-03	1.781E-04	3.576E-05	7.680E-06	1.719E-06	5.712E-05	9.997E-06	2.007E-06	4.331E-07	9.757E-08
4	4.116E-04	7.856E-05	1.639E-05	3.603E-06	8.187E-07					

Table A6. Geometry Coefficients

EPSILON=0.020

		$G_{1m}^e$				$G_{1m}^o$					
		0	1	2	3	4	0	1	2	3	4
OMEGA=0.250											
0	1.571E 00	7.854E-01	5.236E-01	3.927E-01	3.142E-01	6.667E-01	4.0C0E-01	2.857E-01	2.222E-01	1.818E-01	
1	6.667E-01	4.0C0E-01	2.857E-01	2.222E-01	1.818E-01	5.000E-01	3.333E-01	2.500E-01	2.000E-01	1.667E-01	
2	1.475E-08	9.831E-09	7.373E-09	5.898E-09	4.915E-09	1.333E-01	9.524E-02	7.407E-02	6.061E-02	5.128E-02	
3	-1.333E-01	-9.524E-02	-7.407E-02	-6.061E-02	-5.128E-02	-2.518E-08	-1.889E-08	-1.511E-08	-1.259E-08	-1.079E-08	
4	-5.319E-08	-3.989E-08	-3.191E-08	-2.659E-08	-2.280E-08						
OMEGA=0.200											
0	1.257E 00	5.097E-01	2.796E-01	1.750E-01	1.184E-01	4.381E-01	2.0C7E-01	1.105E-01	6.684E-02	4.298E-02	
1	5.169E-01	2.654E-01	1.640E-01	1.115E-01	8.048E-02	3.146E-01	1.685E-01	1.024E-01	6.699E-02	4.605E-02	
2	8.310E-02	6.833E-02	5.661E-02	4.726E-02	3.975E-02	1.222E-01	8.075E-02	5.741E-02	4.260E-02	3.253E-02	
3	-1.014E-02	1.123E-02	1.864E-02	2.073E-02	2.058E-02	5.276E-02	4.291E-02	3.509E-02	2.886E-02	2.387E-02	
4	2.102E-02	1.984E-02	1.853E-02	1.719E-02	1.587E-02						
OMEGA=0.150											
0	9.425E-01	3.070E-01	1.443E-01	8.159E-02	5.195E-02	2.514E-01	8.430E-02	3.584E-02	1.771E-02	9.796E-03	
1	3.787E-01	1.681E-01	9.337E-02	5.884E-02	4.028E-02	1.746E-01	7.436E-02	3.749E-02	2.114E-02	1.295E-02	
2	1.188E-01	7.935E-02	5.521E-02	3.990E-02	2.983E-02	8.981E-02	4.998E-02	3.024E-02	1.941E-02	1.306E-02	
3	5.110E-02	4.450E-02	3.560E-02	2.813E-02	2.239E-02	5.611E-02	3.665E-02	2.472E-02	1.719E-02	1.230E-02	
4	3.825E-02	3.126E-02	2.548E-02	2.086E-02	1.720E-02						
OMEGA=0.100											
0	6.283E-01	1.665E-01	7.276E-02	4.063E-02	2.602E-02	1.133E-01	2.726E-02	9.754E-03	4.522E-03	2.479E-03	
1	2.483E-01	9.744E-02	5.114E-02	3.141E-02	2.123E-02	7.691E-02	2.638E-02	1.178E-02	6.238E-03	3.705E-03	
2	1.089E-01	5.963E-02	3.653E-02	2.438E-02	1.733E-02	4.789E-02	2.179E-02	1.145E-02	6.685E-03	4.227E-03	
3	6.263E-02	4.022E-02	2.709E-02	1.921E-02	1.423E-02	3.409E-02	1.807E-02	1.050E-02	6.571E-03	4.364E-03	
4	4.197E-02	2.891E-02	2.070E-02	1.537E-02	1.179E-02						
OMEGA=0.050											
0	3.142E-01	7.103E-02	3.094E-02	1.737E-02	1.109E-02	2.864E-02	5.174E-03	1.806E-03	8.563E-04	4.770E-04	
1	1.227E-01	4.406E-02	2.255E-02	1.366E-02	9.119E-03	1.917E-02	5.585E-03	2.386E-03	1.248E-03	7.367E-04	
2	6.366E-02	2.981E-02	1.704E-02	1.096E-02	7.589E-03	1.333E-02	5.120E-03	2.494E-03	1.404E-03	8.694E-04	
3	3.968E-02	2.147E-02	1.326E-02	8.936E-03	6.386E-03	9.982E-03	4.513E-03	2.412E-03	1.439E-03	9.269E-04	
4	2.712E-02	1.614E-02	1.057E-02	7.396E-03	5.426E-03						



Table A9. Geometry Coefficients

EPSILON=0.010

		$G_{lm}^e$					$G_{lm}^o$				
$l$	$m$	0	1	2	3	4	0	1	2	3	4
OMEGA=0.250											
0	0	1.571E 00	7.854E-01	5.236E-01	3.927E-01	3.142E-01	6.667E-01	4.000E-01	2.857E-01	2.222E-01	1.818E-01
1	1	6.667E-01	4.000E-01	2.857E-01	2.222E-01	1.818E-01	5.000E-01	3.333E-01	2.500E-01	2.000E-01	1.667E-01
2	2	4.893E-08	3.262E-08	2.447E-08	1.957E-08	1.631E-08	1.333E-01	9.524E-02	7.407E-02	6.061E-02	5.128E-02
3	3	-1.333E-01	-9.524E-02	-7.407E-02	-6.061E-02	-5.128E-02	1.725E-08	-5.044E-08	-4.035E-08	-3.363E-08	-2.882E-08
4	4	-1.188E-07	-8.908E-08	-7.126E-08	-5.938E-08	-5.090E-08					
OMEGA=0.200											
0	0	1.257E 00	5.097E-01	2.796E-01	1.750E-01	1.185E-01	4.381E-01	2.007E-01	1.105E-01	6.684E-02	4.298E-02
1	1	5.169E-01	2.655E-01	1.640E-01	1.115E-01	8.053E-02	3.146E-01	1.685E-01	1.024E-01	6.699E-02	4.605E-02
2	2	8.315E-02	6.838E-02	5.666E-02	4.731E-02	3.980E-02	1.222E-01	8.075E-02	5.742E-02	4.261E-02	3.253E-02
3	3	-1.009E-02	1.127E-02	1.868E-02	2.077E-02	2.062E-02	5.276E-02	4.251E-02	3.509E-02	2.886E-02	2.388E-02
4	4	2.107E-02	1.988E-02	1.858E-02	1.724E-02	1.592E-02					
OMEGA=0.150											
0	0	9.425E-01	3.071E-01	1.443E-01	8.168E-02	5.204E-02	2.513E-01	8.428E-02	3.583E-02	1.770E-02	9.792E-03
1	1	3.788E-01	1.681E-01	9.346E-02	5.894E-02	4.038E-02	1.746E-01	7.434E-02	3.748E-02	2.113E-02	1.295E-02
2	2	1.190E-01	7.945E-02	5.531E-02	4.000E-02	2.993E-02	8.980E-02	4.958E-02	3.024E-02	1.941E-02	1.306E-02
3	3	5.122E-02	4.460E-02	3.570E-02	2.823E-02	2.249E-02	5.611E-02	3.664E-02	2.472E-02	1.719E-02	1.230E-02
4	4	3.836E-02	3.137E-02	2.558E-02	2.096E-02	1.730E-02					
OMEGA=0.100											
0	0	6.283E-01	1.666E-01	7.292E-02	4.081E-02	2.619E-02	1.132E-01	2.724E-02	9.747E-03	4.520E-03	2.479E-03
1	1	2.484E-01	9.760E-02	5.131E-02	3.158E-02	2.141E-02	7.686E-02	2.637E-02	1.177E-02	6.236E-03	3.705E-03
2	2	1.091E-01	5.981E-02	3.671E-02	2.456E-02	1.751E-02	4.787E-02	2.178E-02	1.144E-02	6.684E-03	4.228E-03
3	3	6.283E-02	4.041E-02	2.727E-02	1.939E-02	1.441E-02	3.408E-02	1.807E-02	1.050E-02	6.571E-03	4.366E-03
4	4	4.216E-02	2.910E-02	2.089E-02	1.555E-02	1.196E-02					
OMEGA=0.050											
0	0	3.142E-01	7.135E-02	3.131E-02	1.774E-02	1.145E-02	2.856E-02	5.161E-03	1.804E-03	8.565E-04	4.783E-04
1	1	1.230E-01	4.442E-02	2.292E-02	1.403E-02	9.473E-03	1.912E-02	5.574E-03	2.385E-03	1.250E-03	7.396E-04
2	2	6.402E-02	3.018E-02	1.741E-02	1.132E-02	7.936E-03	1.330E-02	5.114E-03	2.495E-03	1.408E-03	8.743E-04
3	3	4.005E-02	2.184E-02	1.363E-02	9.290E-03	6.726E-03	9.967E-03	4.512E-03	2.416E-03	1.445E-03	9.338E-04
4	4	2.751E-02	1.652E-02	1.093E-02	7.744E-03	5.760E-03					

OMEGA=0.020

0 1.257E-01 2.654E-02 1.182E-02 6.630E-03 4.226E-03 4.602E-03 7.496E-04 2.652E-04 1.249E-04 6.841E-05  
 1 4.886E-02 1.7C3E-02 8.663E-03 5.226E-03 3.482E-03 3.064E-03 8.429E-04 3.545E-04 1.820E-04 1.051E-04  
 2 2.646E-02 1.175E-02 6.611E-03 4.218E-03 2.914E-03 2.471E-03 7.851E-04 3.730E-04 2.046E-04 1.235E-04  
 3 1.675E-02 8.598E-03 5.203E-03 3.471E-03 2.471E-03 2.192E-03 7.029E-04 3.620E-04 2.094E-04 1.312E-04  
 4 1.157E-02 6.554E-03 4.195E-03 2.902E-03 2.120E-03 1.655E-03 7.029E-04 3.620E-04 2.094E-04 1.312E-04

OMEGA=0.010

0 6.278E-02 1.3C3E-02 5.610E-03 3.101E-03 1.949E-03 1.163E-03 1.755E-04 6.081E-05 2.792E-05 1.542E-05  
 1 2.410E-02 8.171E-03 4.083E-03 2.429E-03 1.593E-03 7.615E-04 1.983E-04 8.008E-05 4.071E-05 2.407E-05  
 2 1.297E-02 5.6C2E-03 3.099E-03 1.948E-03 1.320E-03 5.348E-04 1.820E-04 8.366E-05 4.622E-05 2.890E-05  
 3 8.135E-03 4.075E-03 2.427E-03 1.591E-03 1.106E-03 3.945E-04 1.598E-04 8.131E-05 4.810E-05 3.147E-05  
 4 5.578E-03 3.053E-03 1.946E-03 1.319E-03 9.356E-04 3.945E-04 1.598E-04 8.131E-05 4.810E-05 3.147E-05

OMEGA=0.005

0 3.161E-02 6.319E-03 2.611E-03 1.336E-03 7.491E-04 2.975E-04 4.355E-05 1.586E-05 7.841E-06 4.399E-06  
 1 1.189E-02 3.897E-03 1.838E-03 9.924E-04 5.721E-04 1.882E-04 4.975E-05 2.179E-05 1.163E-05 6.745E-06  
 2 6.311E-03 2.610E-03 1.336E-03 7.490E-04 4.410E-04 1.316E-04 4.757E-05 2.352E-05 1.319E-05 7.835E-06  
 3 3.893E-03 1.837E-03 9.921E-04 5.719E-04 3.424E-04 1.316E-04 4.757E-05 2.352E-05 1.319E-05 7.835E-06  
 4 2.607E-03 1.335E-03 7.486E-04 4.408E-04 2.675E-04 9.938E-05 4.355E-05 2.325E-05 1.349E-05 8.151E-06

Table B1

## PENETRATION COEFFICIENTS, SOURCE ENERGY=1.25 MEV, CONCRETE

		COS $\theta_0$ =1.00				COS $\theta_0$ =0.90					
		1	0	1	2	3	4	1	2	3	4
BACKSCATTERING FROM SEMI-INFINITE MEDIUM											
0	8.872E-03	2.312E-03	2.720E-02	-5.630E-02	3.736E-02	9.966E-03	9.515E-03	-2.413E-02	5.471E-02	-3.372E-02	
1	0.	0.	0.	0.	0.	-8.100E-05	4.963E-02	-1.764E-01	2.683E-01	-1.345E-01	
2	0.	0.	0.	0.	0.	-6.878E-04	1.765E-02	-5.611E-02	7.757E-02	-3.508E-02	
3	0.	0.	0.	0.	0.	-1.602E-03	1.668E-02	-4.845E-02	5.992E-02	-2.574E-02	
4	0.	0.	0.	0.	0.	-1.972E-03	2.253E-02	-7.027E-02	8.824E-02	-3.863E-02	
TRANSMISSION, SLAB THICKNESS=1.00 MFP											
0	1.748E-01	-9.291E-01	2.285E 00	-2.524E 00	1.010E 00	9.995E-02	-9.258E-02	-2.752E-01	5.557E-01	-2.763E-01	
1	0.	0.	0.	0.	0.	3.513E-01	-1.375E 00	2.288E 00	-1.818E 00	5.611E-01	
2	0.	0.	0.	0.	0.	3.923E-01	-1.843E 00	3.416E 00	-2.860E 00	8.954E-01	
3	0.	0.	0.	0.	0.	3.426E-01	-1.721E 00	3.309E 00	-2.828E 00	8.974E-01	
4	0.	0.	0.	0.	0.	2.345E-01	-1.228E 00	2.429E 00	-2.130E 00	6.945E-01	
TRANSMISSION, SLAB THICKNESS=2.00 MFP											
0	1.459E-01	-7.863E-01	1.898E 00	-2.050E 00	7.987E-01	7.903E-02	-1.094E-01	-1.487E-01	3.983E-01	-2.156E-01	
1	0.	0.	0.	0.	0.	2.669E-01	-1.146E 00	2.024E 00	-1.671E 00	5.307E-01	
2	0.	0.	0.	0.	0.	2.996E-01	-1.537E 00	3.042E 00	-2.698E 00	8.941E-01	
3	0.	0.	0.	0.	0.	2.592E-01	-1.398E 00	2.825E 00	-2.515E 00	8.281E-01	
4	0.	0.	0.	0.	0.	1.718E-01	-9.351E-01	1.897E 00	-1.676E 00	5.462E-01	
TRANSMISSION, SLAB THICKNESS=3.00 MFP											
0	8.777E-02	-4.996E-01	1.274E 00	-1.450E 00	5.960E-01	4.819E-02	-1.073E-01	3.157E-02	9.856E-02	-6.735E-02	
1	0.	0.	0.	0.	0.	1.486E-01	-7.003E-01	1.308E 00	-1.109E 00	3.530E-01	
2	0.	0.	0.	0.	0.	1.722E-01	-9.312E-01	1.925E 00	-1.768E 00	6.021E-01	
3	0.	0.	0.	0.	0.	1.444E-01	-8.148E-01	1.715E 00	-1.585E 00	5.407E-01	
4	0.	0.	0.	0.	0.	1.037E-01	-5.846E-01	1.221E 00	-1.115E 00	3.760E-01	
TRANSMISSION, SLAB THICKNESS=4.00 MFP											
0	4.775E-02	-2.810E-01	7.134E-01	-7.967E-01	3.186E-01	2.370E-02	-6.208E-02	5.274E-02	3.354E-03	-1.585E-02	
1	0.	0.	0.	0.	0.	7.234E-02	-3.652E-01	7.317E-01	-6.597E-01	2.216E-01	
2	0.	0.	0.	0.	0.	8.179E-02	-4.573E-01	9.663E-01	-8.975E-01	3.069E-01	
3	0.	0.	0.	0.	0.	6.635E-02	-3.902E-01	8.434E-01	-7.942E-01	2.750E-01	
4	0.	0.	0.	0.	0.	4.121E-02	-2.429E-01	5.178E-01	-4.765E-01	1.604E-01	

Table B2

## PENETRATION COEFFICIENTS, SOURCE ENERGY=1.25 MEV, CONCRETE

		COS $\theta_0 = 0.80$					COS $\theta_0 = 0.70$				
		1	2	3	4	0	1	2	3	4	
BACKSCATTERING FROM SEMI-INFINITE MEDIUM											
0	1.118E-02	8.203E-03	-1.168E-02	3.609E-02	-2.118E-02	1.231E-02	-1.704E-03	8.322E-02	-1.510E-01	9.921E-02	
1	2.166E-03	3.626E-02	-1.119E-01	1.769E-01	-8.469E-02	1.415E-02	-8.727E-02	3.821E-01	-5.528E-01	2.911E-01	
2	-1.307E-03	4.196E-02	-1.458E-01	2.057E-01	-9.429E-02	7.749E-03	-7.112E-02	2.728E-01	-3.764E-01	1.900E-01	
3	-1.741E-03	2.375E-02	-7.354E-02	9.607E-02	-4.189E-02	1.909E-03	-1.055E-02	4.039E-02	-5.271E-02	2.941E-02	
4	3.556E-03	-2.014E-02	4.591E-02	-4.426E-02	1.635E-02	-6.621E-03	4.669E-02	-1.187E-01	1.309E-01	-5.020E-02	
TRANSMISSION, SLAB THICKNESS=1.00 MFP											
0	6.564E-02	1.708E-01	-7.780E-01	9.303E-01	-3.764E-01	4.885E-02	1.891E-01	-4.944E-01	3.472E-01	-7.803E-02	
1	2.568E-01	-2.976E-01	-5.994E-01	1.225E 00	-5.800E-01	1.466E-01	4.542E-01	-1.999E 00	2.223E 00	-8.140E-01	
2	3.896E-01	-1.248E 00	1.507E 00	-7.818E-01	1.359E-01	2.410E-01	-5.807E-01	-1.452E 00	2.066E 00	-8.534E-01	
3	4.600E-01	-1.902E 00	3.094E 00	-2.318E 00	6.674E-01	3.454E-01	-7.658E-01	2.096E-01	5.538E-01	-3.420E-01	
4	4.411E-01	-2.044E 00	3.646E 00	-2.939E 00	8.969E-01	4.318E-01	-1.487E 00	1.916E 00	-1.082E 00	2.229E-01	
TRANSMISSION, SLAB THICKNESS=2.00 MFP											
0	4.985E-02	7.077E-02	-4.520E-01	5.228E-01	-1.774E-01	3.438E-02	1.046E-01	-3.859E-01	3.518E-01	-9.609E-02	
1	1.963E-01	-4.707E-01	3.232E-01	-1.573E-02	-2.037E-02	1.102E-01	8.537E-02	-8.593E-01	1.042E 00	-3.687E-01	
2	2.869E-01	-1.120E 00	1.750E 00	-1.302E 00	3.899E-01	1.705E-01	-2.570E-01	-3.055E-01	7.282E-01	-3.320E-01	
3	3.440E-01	-1.602E 00	2.910E 00	-2.417E 00	7.675E-01	2.354E-01	-7.068E-01	6.460E-01	-8.419E-02	-9.010E-02	
4	3.355E-01	-1.658E 00	3.123E 00	-2.637E 00	8.370E-01	2.777E-01	-1.052E 00	1.460E 00	-8.480E-01	1.617E-01	
TRANSMISSION, SLAB THICKNESS=3.00 MFP											
0	2.664E-02	2.942E-02	-2.796E-01	4.139E-01	-1.892E-01	1.737E-02	4.198E-02	-2.251E-01	2.833E-01	-1.160E-01	
1	1.034E-01	-2.795E-01	1.973E-01	6.809E-02	-8.782E-02	5.490E-02	-1.386E-02	-3.422E-01	5.358E-01	-2.325E-01	
2	1.532E-01	-6.487E-01	1.065E 00	-7.900E-01	2.212E-01	8.537E-02	-2.243E-01	1.216E-01	9.994E-02	-8.118E-02	
3	1.788E-01	-8.786E-01	1.653E 00	-1.393E 00	4.406E-01	1.214E-01	-4.790E-01	7.107E-01	-4.698E-01	1.175E-01	
4	1.813E-01	-9.306E-01	1.803E 00	-1.548E 00	4.951E-01	1.425E-01	-6.427E-01	1.105E 00	-8.564E-01	2.519E-01	
TRANSMISSION, SLAB THICKNESS=4.00 MFP											
0	1.323E-02	3.380E-03	-1.070E-01	1.743E-01	-8.346E-02	8.511E-03	8.755E-03	-8.700E-02	1.258E-01	-5.474E-02	
1	4.804E-02	-3.615E-01	1.894E-01	-6.997E-02	-6.103E-03	2.417E-02	-4.068E-02	-5.238E-02	1.390E-01	-6.863E-02	
2	6.895E-02	-3.211E-01	5.777E-01	-4.661E-01	1.405E-01	3.586E-02	-1.233E-01	1.391E-01	-4.564E-02	-5.162E-03	
3	8.445E-02	-4.392E-01	8.646E-01	-7.564E-01	2.468E-01	5.291E-02	-2.365E-01	3.993E-01	-2.996E-01	8.432E-02	
4	8.414E-02	-4.493E-01	8.943E-01	-7.841E-01	2.551E-01	6.152E-02	-3.006E-01	5.547E-01	-4.559E-01	1.405E-01	

Table B3

PENETRATION COEFFICIENTS, SOURCE ENERGY=1.25 MEV, CONCRETE

COS θ<sub>0</sub>=0.60

CCS θ<sub>0</sub>=0.50

	1	0	1	0	1	2	3	4
BACKSCATTERING FROM SEMI-INFINITE MEDIUM								
0	1.359E-02	1.782E-02	-3.008E-02	8.374E-02	-1.378E-03	1.420E-01	-2.592E-01	1.888E-01
1	6.919E-03	4.754E-02	-1.101E-01	1.828E-01	-1.069E-01	5.299E-01	-7.784E-01	4.493E-01
2	4.586E-03	5.956E-03	8.073E-03	-5.638E-03	2.430E-02	5.182E-01	-7.204E-01	3.868E-01
3	2.421E-03	-5.304E-03	3.304E-02	-4.567E-02	3.417E-02	1.450E-02	-1.143E-01	3.960E-01
4	4.220E-03	-1.592E-02	4.004E-02	-4.388E-02	2.464E-02	5.138E-04	-4.193E-03	4.344E-02
TRANSMISSION, SLAB THICKNESS=1.00 MFP								
0	3.872E-02	1.449E-01	-1.380E-01	-1.569E-01	1.266E-01	3.340E-02	3.959E-02	4.380E-01
1	8.630E-02	6.099E-01	-1.682E 00	1.387E 00	-3.849E-01	8.836E-02	1.069E-01	6.175E-01
2	1.249E-01	5.658E-01	-2.087E 00	2.082E 00	-6.771E-01	8.615E-02	3.741E-01	-6.256E-01
3	1.741E-01	3.081E-01	-1.859E 00	2.166E 00	-7.861E-01	7.565E-02	5.959E-01	-1.711E 00
4	2.321E-01	-1.176E-01	-1.037E 00	1.541E 00	-6.170E-01	6.179E-02	7.322E-01	-2.399E 00
TRANSMISSION, SLAB THICKNESS=2.00 MFP								
0	2.573E-02	7.491E-02	-1.913E-01	7.850E-02	2.050E-02	2.026E-02	3.707E-02	-1.945E-02
1	5.762E-02	2.822E-01	-1.076E 00	1.102E 00	-3.577E-01	3.271E-02	2.539E-01	-7.775E-01
2	8.440E-02	1.864E-01	-1.090E 00	1.303E 00	-4.803E-01	3.263E-02	3.316E-01	-1.161E 00
3	1.233E-01	-5.028E-02	-6.769E-01	1.037E 00	-4.318E-01	4.075E-02	3.149E-01	-1.254E 00
4	1.681E-01	-3.660E-01	4.122E-03	4.391E-01	-2.453E-01	5.761E-02	2.038E-01	-1.052E 00
TRANSMISSION, SLAB THICKNESS=3.00 MFP								
0	1.233E-02	2.502E-02	-1.158E-01	1.153E-01	-3.437E-02	8.697E-03	1.462E-02	-5.990E-02
1	2.833E-02	8.088E-02	-4.653E-01	6.020E-01	-2.458E-01	1.495E-02	7.264E-02	-3.253E-01
2	4.197E-02	-3.879E-03	-2.922E-01	4.412E-01	-1.862E-01	1.617E-02	7.465E-02	-3.680E-01
3	5.947E-02	-1.161E-01	-6.487E-02	2.552E-01	-1.337E-01	2.569E-02	1.961E-02	-2.646E-01
4	8.153E-02	-2.702E-01	2.928E-01	-9.301E-02	-1.094E-02	3.458E-02	-4.250E-02	-1.258E-01
TRANSMISSION, SLAB THICKNESS=4.00 MFP								
0	5.570E-03	6.130E-03	-5.242E-02	6.856E-02	-2.783E-02	3.581E-03	4.172E-03	-3.205E-02
1	1.373E-02	-1.671E-03	-3.001E-01	1.574E-01	-6.941E-02	7.264E-03	7.162E-03	-7.714E-02
2	1.786E-02	-3.296E-02	-3.026E-02	9.318E-02	-4.786E-02	6.404E-03	5.316E-03	-7.144E-02
3	2.530E-02	-8.671E-02	9.747E-02	-3.294E-02	-3.132E-03	1.056E-02	-2.108E-02	-1.463E-02
4	3.271E-02	-1.373E-01	2.135E-01	-1.446E-01	3.576E-02	1.378E-02	-4.297E-02	3.619E-02
0	4.252E-02	-1.822E-02	4.252E-02	1.099E-01	-4.828E-02	1.099E-01	-4.828E-02	1.822E-02
1	3.823E-01	-1.442E-01	3.823E-01	-1.442E-01	3.823E-01	-1.442E-01	3.823E-01	-1.442E-01
2	4.587E-01	-1.812E-01	4.587E-01	-1.812E-01	4.587E-01	-1.812E-01	4.587E-01	-1.812E-01
3	3.769E-01	-1.577E-01	3.769E-01	-1.577E-01	3.769E-01	-1.577E-01	3.769E-01	-1.577E-01
4	2.471E-01	-1.134E-01	2.471E-01	-1.134E-01	2.471E-01	-1.134E-01	2.471E-01	-1.134E-01

Table B4

PENETRATION COEFFICIENTS, SOURCE ENERGY=1.25 MEV, CONCRETE

		COS $\theta_0 = 0.40$					COS $\theta_0 = 0.30$				
		1	2	3	4	0	1	2	3	4	
BACKSCATTERING FROM SEMI-INFINITE MEDIUM											
0	1.752E-02	2.040E-02	2.493E-02	-1.395E-02	6.537E-02	1.965E-02	3.445E-C2	-2.077E-03	4.117E-02	9.593E-02	
1	9.904E-03	8.802E-02	-1.846E-01	2.985E-01	-4.657E-02	1.239E-02	1.026E-01	-1.357E-01	1.891E-01	1.278E-01	
2	1.174E-03	8.611E-02	-2.063E-01	2.880E-01	-5.850E-02	8.297E-03	5.316E-C2	-1.359E-02	-1.664E-02	1.767E-01	
3	-2.548E-03	9.133E-02	-2.461E-01	3.123E-01	-8.655E-02	1.366E-02	-4.551E-C2	2.376E-01	-3.349E-01	2.648E-01	
4	6.482E-03	-1.171E-02	3.928E-02	-3.948E-02	4.803E-02	2.039E-02	-1.263E-C1	4.089E-01	-5.044E-01	2.869E-01	
TRANSMISSION, SLAB THICKNESS=1.00 MFP											
0	2.866E-02	2.611E-02	3.455E-01	-6.838E-01	2.970E-01	2.499E-02	-4.782E-C3	4.093E-01	-7.476E-01	3.286E-01	
1	6.627E-02	4.245E-02	7.641E-01	-1.736E-01	8.794E-01	7.260E-02	-2.434E-01	1.657E-01	-2.765E-01	1.295E-01	
2	6.026E-02	2.054E-01	1.029E-01	-9.757E-01	6.181E-01	7.144E-02	-2.118E-01	1.476E-01	-2.578E-01	1.255E-01	
3	3.969E-02	4.426E-01	-8.030E-01	1.790E-01	1.481E-01	5.315E-02	-5.255E-C2	8.529E-01	-1.764E-01	9.183E-01	
4	2.560E-02	5.640E-01	-1.318E-01	8.704E-01	-1.379E-01	2.575E-02	1.480E-C1	1.719E-01	-9.043E-01	5.640E-01	
TRANSMISSION, SLAB THICKNESS=2.00 MFP											
0	1.613E-02	1.962E-02	2.228E-03	-1.133E-01	7.779E-02	1.226E-02	1.232E-02	4.560E-03	-8.692E-02	6.141E-02	
1	2.258E-02	1.530E-01	-3.979E-01	2.420E-01	-1.709E-02	1.461E-02	1.155E-01	-3.005E-01	1.975E-01	-2.261E-02	
2	1.689E-02	2.437E-01	-7.493E-01	7.013E-01	-2.113E-01	9.690E-03	1.658E-01	-4.767E-01	4.117E-01	-1.074E-01	
3	1.096E-02	3.049E-01	-9.883E-01	1.027E-01	-3.546E-01	-1.458E-03	2.383E-01	-6.882E-01	6.662E-01	-2.125E-01	
4	1.272E-02	3.002E-01	-1.029E-01	1.120E-01	-4.040E-01	-9.694E-03	2.731E-C1	-7.778E-01	7.742E-01	-2.579E-01	
TRANSMISSION, SLAB THICKNESS=3.00 MFP											
0	6.359E-03	7.374E-03	-3.350E-02	2.249E-02	-1.652E-03	4.580E-03	4.350E-C3	-2.793E-02	2.989E-02	-1.072E-02	
1	9.342E-03	5.583E-02	-2.330E-01	2.716E-01	-1.039E-01	6.417E-03	2.925E-02	-1.322E-01	1.543E-01	-5.778E-02	
2	7.588E-03	7.490E-02	-3.072E-01	3.722E-01	-1.477E-01	5.616E-03	3.182E-02	-1.445E-01	1.717E-01	-6.476E-02	
3	4.27E-03	5.640E-02	-2.621E-01	3.255E-01	-1.292E-01	4.820E-03	3.746E-02	-1.644E-01	1.998E-01	-7.772E-02	
4	9.546E-03	4.601E-02	-2.346E-01	3.009E-01	-1.219E-01	3.440E-03	3.741E-C2	-1.558E-01	1.879E-01	-7.293E-02	
TRANSMISSION, SLAB THICKNESS=4.00 MFP											
0	2.522E-03	-4.296E-04	-9.990E-03	1.324E-02	-5.296E-03	1.510E-03	1.036E-C3	-1.268E-02	1.917E-02	-8.959E-03	
1	3.577E-03	5.996E-03	-4.652E-02	6.341E-02	-2.650E-02	2.542E-03	1.314E-03	-2.520E-02	3.738E-02	-1.606E-02	
2	4.554E-03	-3.766E-04	-3.519E-02	5.536E-02	-2.437E-02	2.166E-03	4.032E-03	-3.591E-02	5.413E-02	-2.441E-02	
3	4.965E-03	-5.673E-03	-2.282E-02	4.425E-02	-2.073E-02	3.346E-03	-5.039E-C3	-9.079E-03	2.089E-02	-1.013E-02	
4	6.906E-03	-1.850E-02	6.531E-03	1.587E-02	-1.082E-02	2.281E-03	-7.752E-C4	-1.681E-02	2.817E-02	-1.287E-02	

Table B5

PENETRATION COEFFICIENTS, SOURCE ENERGY=1.25 MEV, CONCRETE

m	COS $\theta_0 = 0.20$					COS $\theta_0 = 0.10$					
	1	0	1	2	3	4	0	1	2	3	4
BACKSCATTERING FROM SEMI-INFINITE MEDIUM											
0	2.362E-02	-2.969E-02	5.142E-01	-1.003E-01	8.310E-01	2.960E-02	-2.965E-01	2.387E-00	-4.837E-00	3.400E-00	
1	6.766E-02	-5.270E-01	2.462E-00	-3.775E-00	2.319E-00	2.393E-01	-2.688E-00	1.125E-01	-1.734E-01	9.678E-00	
2	9.193E-02	-8.453E-01	3.248E-00	-4.586E-00	2.489E-00	3.328E-01	-3.432E-00	1.263E-01	-1.793E-01	9.244E-00	
3	1.091E-01	-9.436E-01	3.166E-00	-4.134E-00	2.068E-00	4.411E-01	-4.056E-00	1.328E-01	-1.742E-01	8.338E-00	
4	9.399E-02	-7.787E-01	2.424E-00	-3.004E-00	1.436E-00	5.262E-01	-4.404E-00	1.320E-01	-1.623E-01	7.306E-00	
TRANSMISSION, SLAB THICKNESS=1.00 MFP											
0	2.093E-02	-1.658E-02	3.708E-01	-6.626E-01	2.935E-01	1.787E-02	-2.137E-02	3.103E-01	-6.137E-01	3.107E-01	
1	6.150E-02	-2.845E-01	1.612E-00	-2.553E-00	1.171E-00	4.759E-02	-2.444E-01	1.270E-00	-2.055E-00	9.841E-01	
2	6.208E-02	-2.946E-01	1.558E-00	-2.480E-00	1.161E-00	4.112E-02	-2.349E-01	1.177E-00	-1.879E-00	8.966E-01	
3	5.517E-02	-2.412E-01	1.255E-00	-2.040E-00	9.739E-01	3.308E-02	-1.882E-01	9.521E-01	-1.528E-00	7.312E-01	
4	3.886E-02	-1.356E-01	8.497E-01	-1.488E-00	7.373E-01	1.866E-02	-9.755E-02	6.481E-01	-1.124E-00	5.554E-01	
TRANSMISSION, SLAB THICKNESS=2.00 MFP											
0	9.723E-03	4.470E-03	8.918E-03	-7.488E-02	5.371E-02	7.050E-03	-2.535E-03	3.081E-02	-9.860E-02	6.687E-02	
1	1.335E-02	4.359E-02	-9.369E-02	-2.517E-02	6.411E-02	9.668E-03	1.878E-02	-4.498E-02	-2.208E-02	4.060E-02	
2	6.930E-03	9.595E-02	-2.729E-01	2.139E-01	-4.235E-02	3.215E-03	6.157E-02	-1.844E-01	1.675E-01	-4.764E-02	
3	2.758E-03	1.145E-01	3.334E-01	2.996E-01	-8.244E-02	-4.111E-03	9.638E-02	-2.694E-01	2.644E-01	-8.726E-02	
4	-4.056E-03	1.486E-01	-4.236E-01	4.128E-01	-1.329E-01	-1.134E-02	1.400E-01	-3.794E-01	3.873E-01	-1.369E-01	
TRANSMISSION, SLAB THICKNESS=3.00 MFP											
0	3.458E-03	-5.288E-03	2.304E-02	-5.807E-02	3.922E-02	2.092E-03	-1.190E-03	2.250E-03	-1.264E-02	1.094E-02	
1	5.827E-03	-1.810E-04	-2.122E-02	1.043E-02	6.151E-03	2.419E-03	6.292E-03	-3.840E-02	5.013E-02	-2.045E-02	
2	5.080E-03	1.121E-02	-7.200E-02	9.041E-02	-3.460E-02	-7.015E-04	2.684E-02	-9.914E-02	1.286E-01	-5.657E-02	
3	7.601E-03	-1.305E-02	-8.951E-04	6.030E-03	8.538E-04	1.873E-04	1.325E-02	-4.756E-02	5.545E-02	-2.136E-02	
4	7.628E-03	-1.068E-02	-1.885E-02	3.933E-02	-1.732E-02	-3.723E-04	1.466E-02	-4.678E-02	5.112E-02	-1.855E-02	
TRANSMISSION, SLAB THICKNESS=4.00 MFP											
0	9.409E-04	-4.572E-04	-3.371E-03	6.009E-03	-3.109E-03	5.948E-04	1.407E-04	-4.052E-03	6.091E-03	-2.774E-03	
1	1.324E-03	-3.138E-04	-9.630E-03	1.535E-02	-6.724E-03	9.050E-04	-1.038E-03	-3.118E-03	5.743E-03	-2.503E-03	
2	1.508E-03	-2.046E-03	-6.341E-03	1.287E-02	-5.989E-03	2.905E-05	1.951E-03	-8.189E-03	1.092E-02	-4.717E-03	
3	1.732E-03	-4.496E-03	3.889E-04	5.699E-03	-3.322E-03	-6.880E-06	1.854E-03	-7.455E-03	9.646E-03	-4.042E-03	
4	2.105E-03	-6.907E-03	6.351E-03	-1.856E-04	-1.364E-03	-2.232E-04	3.064E-04	-9.573E-03	1.109E-02	-4.361E-03	

Table 56

PENETRATION COEFFICIENTS, SOURCE ENERGY=1.25 MEV, CONCRETE

CCS $\theta_0$ =0.01

m	0	1	2	3	4
	BACKSCATTERING FROM SEMI-INFINITE MEDIUM				
0	1.385E-01	-6.520E 00	4.267E 01	-8.491E 01	5.239E 01
1	4.541E 00	-5.796E 01	2.265E 02	-3.395E 02	1.730E 02
2	6.855E 00	-7.467E 01	2.608E 02	-3.603E 02	1.723E 02
3	9.332E 00	-8.765E 01	2.756E 02	-3.527E 02	1.588E 02
4	1.102E 01	-9.262E 01	2.682E 02	-3.225E 02	1.382E 02
	TRANSMISSION, SLAB THICKNESS=1.00 MFP				
0	1.438E-02	-3.784E-03	1.442E-01	-3.189E-01	1.664E-01
1	3.168E-02	-1.135E-01	6.432E-01	-1.119E 00	5.602E-01
2	2.530E-02	-1.156E-01	6.270E-01	-1.064E 00	5.299E-01
3	1.810E-02	-9.275E-02	5.194E-01	-8.834E-01	4.403E-01
4	9.242E-03	-4.551E-02	3.556E-01	-6.497E-01	3.316E-01
	TRANSMISSION, SLAB THICKNESS=2.00 MFP				
0	4.820E-03	2.460E-03	-1.105E-02	-1.957E-03	7.623E-03
1	4.361E-03	2.991E-02	-1.083E-01	1.139E-01	-3.928E-02
2	4.783E-04	4.270E-02	-1.346E-01	1.395E-01	-4.782E-02
3	-1.938E-03	4.861E-02	-1.385E-01	1.373E-01	-4.494E-02
4	-5.453E-03	6.703E-02	-1.791E-01	1.795E-01	-6.183E-02
	TRANSMISSION, SLAB THICKNESS=3.00 MFP				
0	1.247E-03	1.570E-04	-7.073E-03	9.684E-03	-3.788E-03
1	1.571E-03	3.756E-03	-2.310E-02	2.982E-02	-1.173E-02
2	9.204E-04	4.997E-03	-2.326E-02	2.867E-02	-1.111E-02
3	8.706E-04	5.045E-03	-2.282E-02	2.760E-02	-1.055E-02
4	8.103E-04	4.661E-03	-2.137E-02	2.607E-02	-1.007E-02
	TRANSMISSION, SLAB THICKNESS=4.00 MFP				
0	6.356E-04	-5.134E-04	-2.196E-03	4.407E-03	-2.335E-03
1	4.995E-04	6.789E-04	-7.293E-03	1.167E-02	-5.578E-03
2	3.406E-04	3.207E-04	-4.840E-03	7.909E-03	-3.735E-03
3	2.902E-04	-1.333E-04	-2.237E-03	3.799E-03	-1.721E-03
4	6.325E-04	-2.170E-03	2.394E-03	-8.309E-04	-2.596E-05

Table B7

PENETRATION COEFFICIENTS, SOURCE ENERGY=0.66 MEV, CONCRETE

$\text{CCS}\theta_0=0.50$

$\text{COS}\theta_0=1.00$

$\mu$	0	1	2	3	4	0	1	2	3	4
BACKSCATTERING FROM SEMI-INFINITE MEDIUM										
0	1.522E-02	8.156E-03	-1.157E-02	2.854E-02	-1.931E-02	2.465E-02	1.787E-02	4.926E-02	-5.771E-02	7.096E-02
1	0.	0.	0.	0.	0.	1.496E-02	7.610E-03	1.026E-01	-1.217E-01	1.200E-01
2	0.	0.	0.	0.	0.	7.682E-03	2.834E-03	4.889E-02	-4.488E-02	5.404E-02
3	0.	0.	0.	0.	0.	2.498E-03	3.788E-03	2.038E-02	-1.418E-02	2.168E-02
4	0.	0.	0.	0.	0.	6.473E-03	-2.896E-02	8.165E-02	-8.175E-02	3.820E-02
TRANSMISSION, SLAB THICKNESS=1.00 MFP										
0	1.340E-01	-4.833E-01	9.866E-01	-1.016E 00	3.966E-01	4.328E-02	7.791E-02	6.931E-02	-3.271E-01	1.626E-01
1	0.	0.	0.	0.	0.	9.677E-02	9.570E-02	6.126E-02	-6.074E-01	3.832E-01
2	0.	0.	0.	0.	0.	1.014E-01	6.676E-02	-1.717E-01	-1.687E-01	1.899E-01
3	0.	0.	0.	0.	0.	9.209E-02	1.301E-02	-2.241E-01	7.859E-02	4.865E-02
4	0.	0.	0.	0.	0.	6.027E-02	5.241E-02	-3.534E-01	3.284E-01	-8.447E-02
TRANSMISSION, SLAB THICKNESS=2.00 MFP										
0	1.162E-01	-4.220E-01	8.533E-01	-8.789E-01	3.458E-01	2.960E-02	3.478E-02	-6.080E-02	-7.212E-02	8.272E-02
1	0.	0.	0.	0.	0.	5.253E-02	9.535E-02	-3.848E-01	2.913E-01	-4.503E-02
2	0.	0.	0.	0.	0.	5.014E-02	7.388E-02	-4.459E-01	4.802E-01	-1.540E-01
3	0.	0.	0.	0.	0.	4.099E-02	4.861E-02	-4.007E-01	5.053E-01	-1.936E-01
4	0.	0.	0.	0.	0.	2.533E-02	6.116E-02	-3.817E-01	4.947E-01	-2.007E-01
TRANSMISSION, SLAB THICKNESS=3.00 MFP										
0	7.036E-02	-2.703E-01	5.552E-01	-5.738E-01	2.275E-01	1.561E-02	9.203E-03	-6.890E-02	6.514E-02	-1.605E-02
1	0.	0.	0.	0.	0.	2.464E-02	2.408E-02	-2.234E-01	2.959E-01	-1.191E-01
2	0.	0.	0.	0.	0.	2.171E-02	8.161E-03	-1.928E-01	2.884E-01	-1.268E-01
3	0.	0.	0.	0.	0.	1.845E-02	-1.224E-02	-1.124E-01	1.968E-01	-9.172E-02
4	0.	0.	0.	0.	0.	1.329E-02	-8.391E-03	-8.626E-02	1.524E-01	-7.173E-02
TRANSMISSION, SLAB THICKNESS=4.00 MFP										
0	3.922E-02	-1.514E-01	3.088E-01	-3.123E-01	1.203E-01	7.226E-03	-3.090E-03	-2.376E-02	3.278E-02	-1.132E-02
1	0.	0.	0.	0.	0.	1.083E-02	-7.845E-03	-5.045E-02	8.867E-02	-4.060E-02
2	0.	0.	0.	0.	0.	1.122E-02	-2.042E-02	-1.594E-02	5.477E-02	-2.930E-02
3	0.	0.	0.	0.	0.	9.106E-03	-2.462E-02	9.889E-03	2.145E-02	-1.594E-02
4	0.	0.	0.	0.	0.	8.099E-03	-2.811E-02	3.056E-02	-7.008E-03	-3.576E-03

Table B8

## PENETRATION COEFFICIENTS, SOURCE ENERGY=0.66 MEV, IRON

		CGS $\theta_0 = 1.00$				CGS $\theta_0 = 0.50$				
		1	2	3	4	0	1	2	3	4
BACKSCATTERING FROM SEMI-INFINITE MEDIUM										
0	9.450E-03	3.849E-03	2.469E-03	6.124E-03	-6.867E-03	1.861E-02	1.829E-02	2.431E-02	1.354E-03	2.938E-02
1	0.	0.	0.	0.	0.	1.396E-02	2.225E-02	3.721E-02	-9.638E-03	5.468E-02
2	0.	0.	0.	0.	0.	8.510E-03	2.838E-02	5.518E-02	-5.286E-02	5.761E-02
3	0.	0.	0.	0.	0.	2.974E-03	-2.410E-03	4.239E-02	-4.954E-02	4.025E-02
4	0.	0.	0.	0.	0.	7.134E-03	-3.780E-02	1.081E-01	-1.169E-01	5.506E-02
TRANSMISSION, SLAB THICKNESS=1.00 MFP										
0	1.313E-01	-4.853E-01	1.008E 00	-1.053E 00	4.202E-01	3.794E-02	6.951E-02	8.038E-02	-3.437E-01	1.694E-01
1	0.	0.	0.	0.	0.	9.441E-02	9.954E-02	4.138E-02	-5.731E-01	3.557E-01
2	0.	0.	0.	0.	0.	1.020E-01	5.001E-02	-1.400E-01	-1.867E-01	1.862E-01
3	0.	0.	0.	0.	0.	9.093E-02	1.373E-02	-2.307E-01	1.005E-01	3.148E-02
4	0.	0.	0.	0.	0.	7.119E-02	-2.259E-03	-2.425E-01	2.316E-01	-5.513E-02
TRANSMISSION, SLAB THICKNESS=2.00 MFP										
0	1.087E-01	-4.381E-01	9.230E-01	-9.778E-01	3.987E-01	2.452E-02	2.828E-02	-4.602E-02	-8.239E-02	8.309E-02
1	0.	0.	0.	0.	0.	4.978E-02	9.448E-02	3.851E-01	2.929E-01	-4.510E-02
2	0.	0.	0.	0.	0.	5.255E-02	5.364E-02	-4.058E-01	4.465E-01	-1.441E-01
3	0.	0.	0.	0.	0.	4.276E-02	4.069E-02	-3.861E-01	4.911E-01	-1.879E-01
4	0.	0.	0.	0.	0.	3.754E-02	-4.009E-03	-2.390E-01	3.491E-01	-1.438E-01
TRANSMISSION, SLAB THICKNESS=3.00 MFP										
0	6.572E-02	-2.858E-01	6.085E-01	-6.324E-01	2.500E-01	1.057E-02	7.139E-03	-5.821E-02	5.659E-02	-1.422E-02
1	0.	0.	0.	0.	0.	1.954E-02	2.934E-02	-2.254E-01	2.975E-01	-1.208E-01
2	0.	0.	0.	0.	0.	2.190E-02	-2.947E-03	-1.571E-01	2.440E-01	-1.060E-01
3	0.	0.	0.	0.	0.	2.086E-02	-2.158E-02	-9.301E-02	1.781E-01	-8.452E-02
4	0.	0.	0.	0.	0.	1.911E-02	-3.659E-02	-2.833E-02	9.767E-02	-5.217E-02
TRANSMISSION, SLAB THICKNESS=4.00 MFP										
0	3.595E-02	-1.612E-01	3.597E-01	-3.913E-01	1.602E-01	4.542E-03	-1.748E-03	-2.071E-02	3.342E-02	-1.501E-02
1	0.	0.	0.	0.	0.	8.546E-03	-4.627E-03	-5.495E-02	9.706E-02	-4.630E-02
2	0.	0.	0.	0.	0.	1.057E-02	-2.320E-02	-6.938E-03	4.747E-02	-2.806E-02
3	0.	0.	0.	0.	0.	1.046E-02	-3.163E-02	2.421E-02	7.935E-03	-1.112E-02
4	0.	0.	0.	0.	0.	1.134E-02	-4.619E-02	6.969E-02	-4.557E-02	1.072E-02

Table B9

## Penetration Coefficients for 1.25 Mev Plane Isotropic Source

Slab Thickness (mfp) \ i	0	1	2	3	4
Scattered Radiation					
1.0	0.02328	0.002676	0.05927	-0.1664	0.08758
2.0	0.01609	-0.004581	-0.02433	0.007650	0.007906
3.0	0.008504	-0.009614	-0.01102	0.02212	-0.009066
4.0	0.004075	-0.007605	0.0005644	0.008656	-0.005422
Scattered Radiation + Unscattered Radiation					
1.0	0.05277	-0.01522	0.1846	-0.5183	0.3030
2.0	0.02678	-0.01019	-0.06889	0.06644	-0.01124
3.0	0.01246	-0.01677	-0.02044	0.04773	-0.02209
4.0	0.005538	-0.01228	0.003480	0.01156	-0.008053